



NRL/FR/5324-93-9536

Characteristics of High-Frequency Signals, Noise, Availability, and Duration of Bandwidths Based on ROTH Amchitka Spectrum Measurements

G. D. McNEAL

*Advanced Radar Systems
Radar Division*

April 16, 1993

UNCLASSIFIED

REPORT DOCUMENTATION PAGE			<i>Form Approved</i> <i>OMB No. 0704-0188</i>	
Public reporting burden for this collection of information is estimated to average 1 hour per response, including the time for reviewing instructions, searching existing data sources, gathering and maintaining the data needed, and completing and reviewing the collection of information. Send comments regarding this burden estimate or any other aspect of this collection of information, including suggestions for reducing this burden, to Washington Headquarters Services, Directorate for Information Operations and Reports, 1215 Jefferson Davis Highway, Suite 1204, Arlington, VA 22202-4302, and to the Office of Management and Budget, Paperwork Reduction Project (0704-0188), Washington, DC 20503.				
1. AGENCY USE ONLY (Leave Blank)	2. REPORT DATE April 16, 1993	3. REPORT TYPE AND DATES COVERED Interim		
4. TITLE AND SUBTITLE Characteristics of High-Frequency Signals, Noise, Availability, and Duration of Bandwidths Based on ROTHRA Amchitka Spectrum Measurements			5. FUNDING NUMBERS PE - OMN, 204577N WU - DN291-215 TA - 148-NRL-92-VARI-002	
6. AUTHOR(S) G.D. Mc Neal			8. PERFORMING ORGANIZATION REPORT NUMBER NRL/FR/5324-92-9536	
7. PERFORMING ORGANIZATION NAME(S) AND ADDRESS(ES) Naval Research Laboratory Washington, DC 20375-5320			9. SPONSORING/MONITORING AGENCY NAME(S) AND ADDRESS(ES) Space and Naval Warfare Systems Command PMW-148 Washington, DC 20363-5100	
11. SUPPLEMENTARY NOTES			10. SPONSORING/MONITORING AGENCY REPORT NUMBER	
12a. DISTRIBUTION/AVAILABILITY STATEMENT Approved for public release; distribution unlimited.			12b. DISTRIBUTION CODE	
13. ABSTRACT (<i>Maximum 200 words</i>) The successful performance of a High-Frequency (HF) Over-The-Horizon Radar (OTHRA) is dependent upon the environment in which the radar must operate. This study investigates measured power levels of noise and signal characteristics in the HF environment of an operational OTHRA system located in Amchitka, Alaska. These measurements were acquired by the Navy's AN/TPS-71 Relocatable OTHRA (ROTHRA) spectrum monitor, and represent a new source of HF environmental measurements for noise characteristics, channel availability, and expected duration of various channel widths as a function of frequency, time-of-day, and season-of-year. The analysis and results presented are based on HF environmental measurements obtained over the 5 to 28 MHz frequency band by a receiver with a very low noise figure, an efficient antenna, a high dynamic range, and which was seldom internally noise limited. The analysis of this data has provided information on power levels associated with noise and HF users in the geographic region of the radar. Clear channel availability results are based on a threshold level defined by empirical distribution functions (EDF) of the measured power levels from the ROTHRA site in Amchitka. Discussions are also provided on how the noise power levels measured by the spectrum monitor compare with CCIR predictions for this geographical location. Directional characteristics are inferred by comparing spectrum monitor noise levels with those seen on the radar.				
14. SUBJECT TERMS HF Noise HF Channel Widths HF Channel Durations			15. NUMBER OF PAGES 44	
17. SECURITY CLASSIFICATION OF REPORT UNCLASSIFIED			16. PRICE CODE	
18. SECURITY CLASSIFICATION OF THIS PAGE UNCLASSIFIED		19. SECURITY CLASSIFICATION OF ABSTRACT UNCLASSIFIED		20. LIMITATION OF ABSTRACT UL

CHARACTERISTICS OF HIGH-FREQUENCY SIGNALS, NOISE, AVAILABILITY, AND DURATION OF BANDWIDTHS BASED ON ROTH AMCHITKA SPECTRUM MEASUREMENTS

1. INTRODUCTION

The development and operational deployment of HF radars has provided an opportunity to examine the HF band with greater measurement accuracy than is available with conventional test equipment and in greater detail than would otherwise be likely [1]. Such radars continually select frequencies and adapt waveforms to fit the existing HF environment, and part of this procedure evolves regular and frequent scans of a large span of the HF band. The exceptional features of radar operations that are being exploited in this analysis are principally derived from the radar's spectrum monitor (SM) subsystem. The spectrum monitor is capable of linearly recording both the strongest HF band signals and the environmental noise in an unused channel — a feature not possible with commercial test equipment. The basic data being analyzed are records of power level at the terminals of a wide azimuthal beamwidth antenna made in narrowband steps between 5 and 28 MHz. The data records were acquired by the Navy's AN/TPS-71 Relocatable Over-The-Horizon Radar (ROTHR) system. The ROTHR is an operational landbased HF (5 to 28 MHz) radar system geographically located on Amchitka Island, Alaska. The primary mission of the ROTHR is to support maritime anti-air and anti-surface warfare for Naval tactical forces in selected operating areas. In addition, the ROTHR is required to perform this mission on a not-to-interfere basis.

The objective of this analysis is to take advantage of the ROTHR data collected from operations on Amchitka Island to investigate

- (a) maximum signal levels with which the ROTHR must coexist,
- (b) how the CCIR (International Radio Consultative Committee) noise model compares with SM measured data (i.e., if noise measurements from the SM and radar are indicated directionally; and if the radar is self-noise-limited),
- (c) maximum and minimum power levels to identify dynamic range requirements,
- (d) channel availability based on SM measurements, and determination of the fraction of available channels as a function of bandwidth,
- (e) lifetimes of available channels.

Section 2 presents a description of the equipment and data characteristics. Section 3 provides results and analysis based on empirical noise power distributions of the HF environment at the ROTHR site. Sections 4 and 5 compare the noise estimates based on SM data with CCIR noise predictions, the radar's specified minimum noise level, and the narrow azimuthal beam width radar. Plots indicate times and frequency bands where the ROTHR is expected to be limited by internal noise. Results from Sections 4 and 5 agree with Nichols and Gooding [2], and the CCIR model [3]. Section 6 discusses the decision rule for channel availability and processing method. Section 7 describes how available channel widths are determined, and plots the availability of selected channel widths for each MHz frequency interval from 5 to 28 MHz during day and nighttime operations. Results of bandwidth duration are given for January

and July in Section 8, representing the seasons that will most likely show a noticeable difference in duration characteristics. Section 9 presents conclusions of the investigation.

SM data acquired during the hours of 00-GMT (00Z) and 12-GMT (12Z) were used for the investigation of channel availability. These times, 00Z (local daytime) and 12Z (local nighttime), represent day and nighttime respectively at the radar site, and also can be considered respectively as a best- and worst-case scenario to determine the number of available channels that could be used by the radar. Results of the analysis indicate frequency regions in the HF spectrum where available channels may be found during day and nighttime ROTHr operations at the Amchitka location.

2. EQUIPMENT AND DATA DESCRIPTION

The noise data analyzed in this study was obtained by the ROTHr spectrum monitor, a passive subsystem of the ROTHr radar. The receive antenna of the SM is a Twin-Whip Endfire Receiving Pair (TWERP) monopole pair. This type of antenna was developed by SRI [4]. The TWERP monopoles are 17 ft high, and have a diameter of 6 in. at the base which tapers to a 3 in. diameter at the top. The front-to-back separation of the antenna poles is 13.8 ft, the monopoles are matched to a 200 ohm transformer by a 3 dB 180 degree hybrid with an equivalent 3.29 meter delay line in the front leg. In addition, there is 100 ft of ground screen in front of the pole and 20 ft of ground screen behind the back pole to enhance the front to back ratio. The SM receiver has a 14.5 dB noise figure, an equivalent noise bandwidth of 4.5 KHz, and a linear dynamic range of 110 dB. The power levels measured at the terminals of the receive antenna are digitized at a 2.5 MHz rate using a 16-bit A/D converter before being passed to the environment signal processor (ESP). Figure 1 shows a simplified diagram of the SM receiver setup. Figure 2 provides a description of the TWERP configuration and a simplified representation of the end-fire beam pattern. Figure 3 provides a plot of the receive antenna's front-to-back ratio, Fig. 4 indicates the E Field (azimuthal) pattern of the antenna, and Table 1 indicates the directivity of the endfire receive antenna for various elevation angles vs frequency.

2.1 Spectrum Monitor Data Description

The HF spectrum data are updated by the ROTHr system approximately every 25 s. The data samples in each update represent the power level in each 3 KHz channel of the HF spectrum from 5 MHz to 28 MHz, the operating frequency range of the ROTHr. To analyze an update for noise estimates, each update is partitioned into 23 segments (333 points per segment) where each segment represents a 1 MHz analysis interval in the 5 to 28 MHz band. Within each analysis interval, the channel with the lowest power level is used as the noise estimate for that given update. Figure 5(a) is an example of the 7667 power levels of the 3 KHz channels acquired during a single spectrum update. Figures 5(b) and (c) compare the statistics (upper, median, and lower deciles) of the noise estimates based on a 100 KHz and 1 MHz analysis interval, respectively. Smaller variations between the amplitudes of the estimates are obtained when a 1 MHz analysis interval is used, and the estimates based on this interval reflect the characteristics of the noise floor indicated by the top display of Fig. 5. Therefore, a 1 MHz analysis interval is used to obtain estimates of the noise floor for all SM data analyzed in this study.

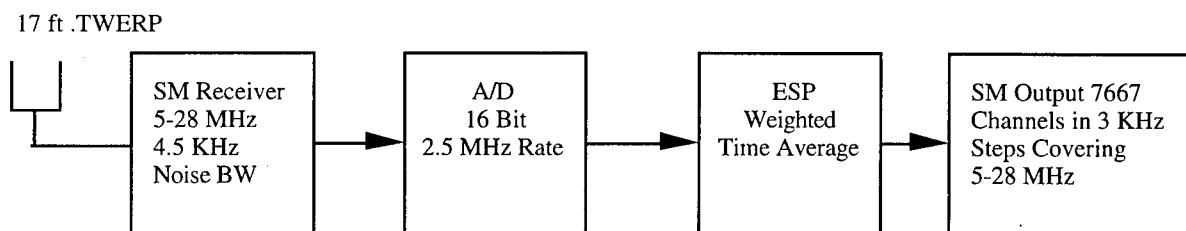


Fig. 1 — Block diagram of SM receiver setup

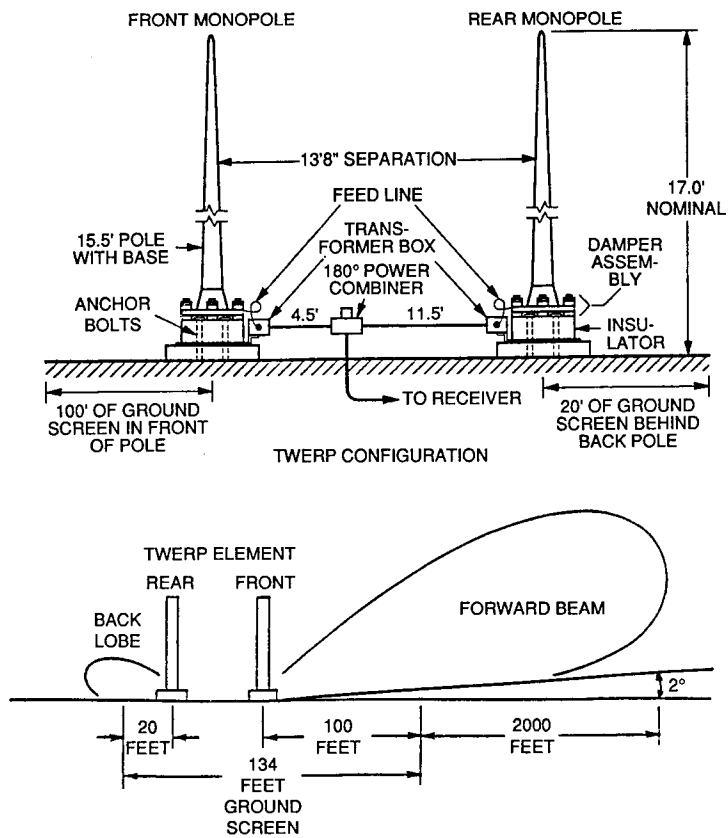


Fig. 2 — Antenna configuration and beam pattern (drawing by Raytheon)

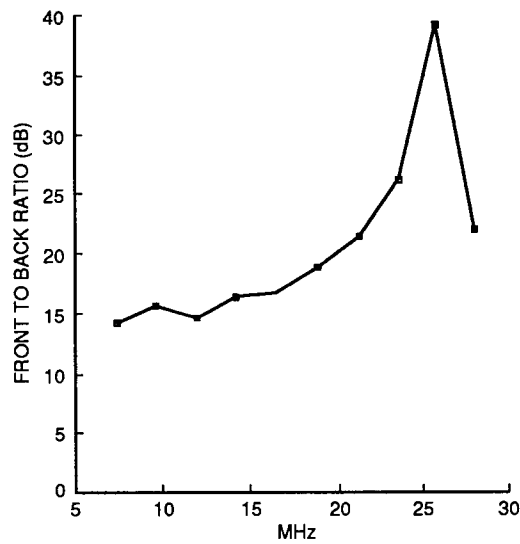
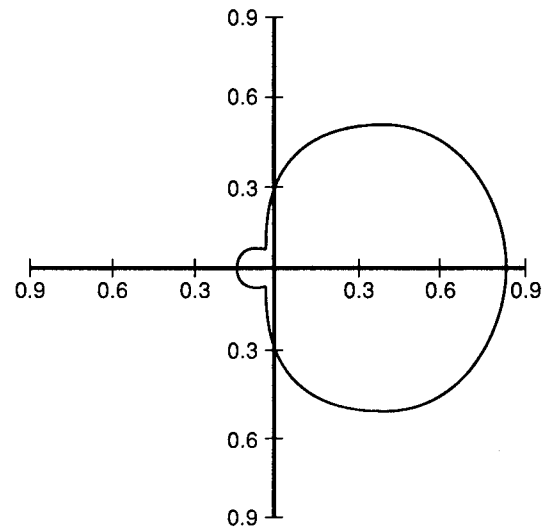


Fig. 3 — Antenna front-to-back ratio vs frequency (graph by Raytheon)

FAR-FIELD GROUND
 $\sigma = 5.0$ mS
 $t_p = 15.0$

Frequency = 16.500 MHz
 Azimuthal Plane
 $\theta = 80.00$ deg

E FIELD PATTERN



Rear Groundscreen
 Length = 7.00 meters

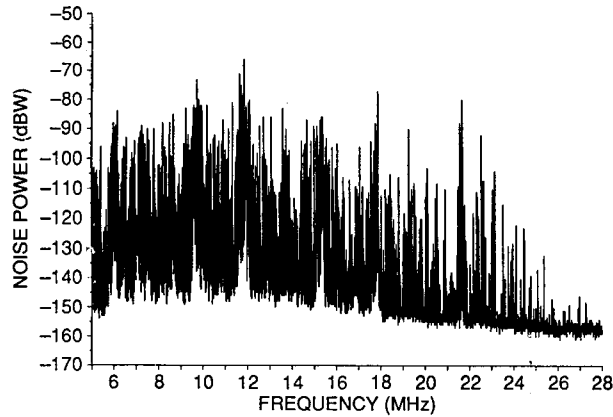
Front Groundscreen
 Length = 33.33 meters

Without Diffraction
 With Segment Splitting

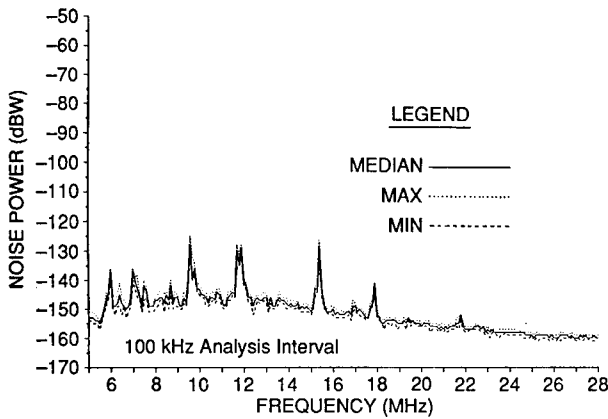
Fig. 4 — E field (azimuthal) pattern of receive antenna
 (drawing by Raytheon)

Table 1 — Spectrum Monitor Antenna Directivity (dB) for Elevation vs Frequency

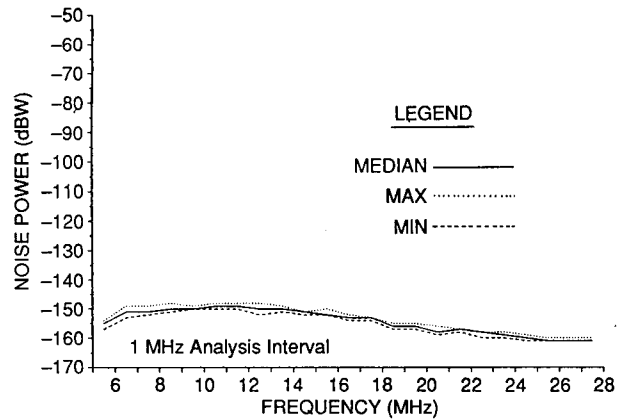
Elevation Angle Degrees	FREQUENCY IN MHz						
	5	8	12	16	20	24	28
2	-2.5	-0.5	0.5	0.5	1.3	1.3	0.1
4	1.5	3.5	4.5	5.5	7.3	7.3	7.1
6	2.5	5.5	6.5	7.5	9.3	9.3	11.1
8	3.5	5.5	7.5	8.5	10.3	11.3	12.1
10	3.5	5.5	7.5	8.5	10.3	11.3	12.1
14	3.5	5.5	7.5	7.5	10.3	10.3	12.1
18	3.5	5.5	7.5	7.5	10.3	10.3	11.1
22	2.5	4.5	6.5	7.5	9.3	9.3	11.1
26	2.5	4.5	6.5	6.5	9.3	9.3	10.1



(a)



(b)



(c)

Fig. 5 — Interval of noise analysis

Historically, analysis of HF data indicates stability in the noise levels with respect to a given time of day and season [3 and 5]. To determine if SM measurements are stable for a given time period, upper deciles, medians, and lower deciles based on minimum power levels in analysis intervals were generated for time periods of 3 minutes and 1 hour. Figure 6 compares the noise statistics of these time periods. Observe that the most noticeable difference in the statistics of the two data sets is in the spread of the upper and lower deciles about the median curve. Also note that the curves representing the median of the minimum power levels (MEOMI), shown by the solid lines, are in good agreement, i.e., small variability in amplitude vs frequency. These characteristics were typical of the data analyzed, and indicate that the MEOMI provides an estimate of the noise that has characteristic behavior as indicated by historical data.

To verify the results associated with the MEOMI for a larger segment of the time interval, SM data was analyzed over a 30 minute period and compared with the MEOMIs based on the 1 hour time period. In addition to computing the MEOMIs, statistics associated with the maximum signal in an analysis interval were also incorporated. Results of the analysis are presented in Fig. 7, where the upper decile, median, and lower decile associated with the MEOMI, and the median of the maximum power levels (MEOMA) are plotted. These plots indicate that the MEOMIs based on the 30-minute data set are in good agreement with those based on the 1 hour data set. Also observe that the MEOMAs from the two time periods are in good agreement, and these results are consistent with those obtained from the data presented in Fig. 6. Furthermore, Fig. 7 indicates the dynamic range of the signal levels in the Amchitka HF environment in which the ROTHM must operate during the indicated time and season of year.

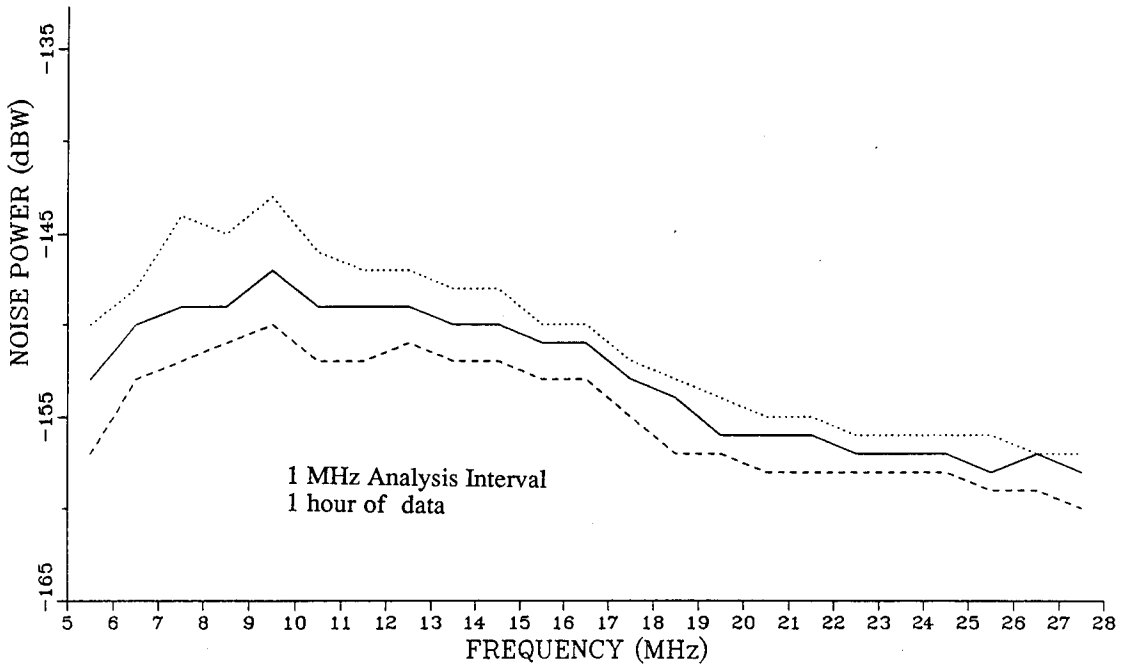
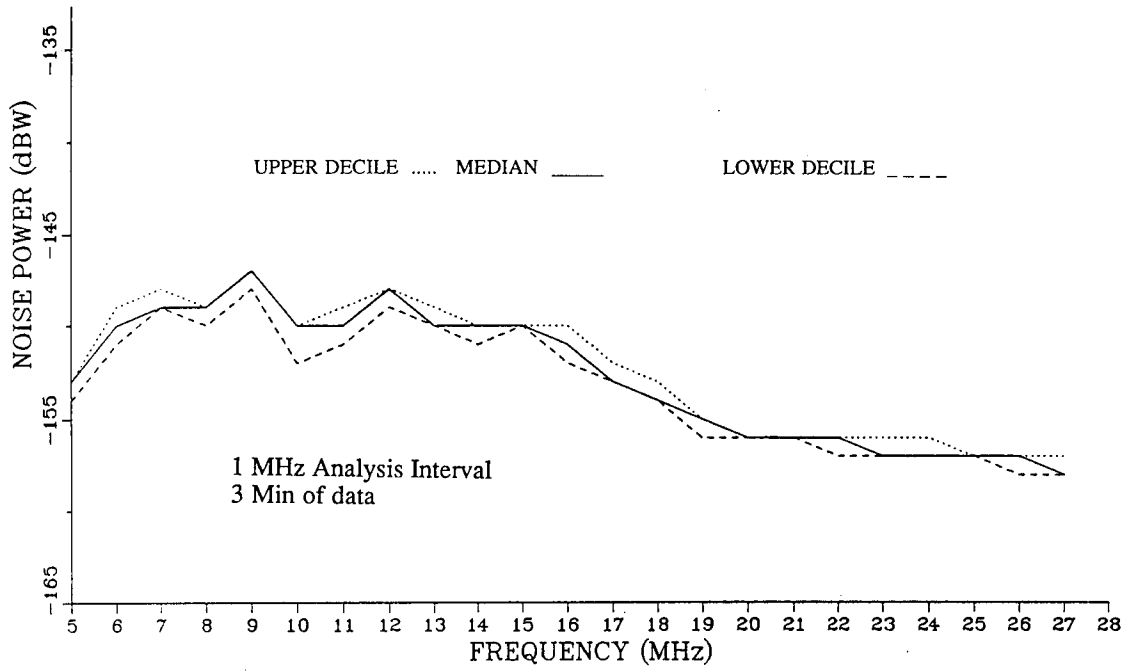


Fig. 6 — ROTH noise, Amchitka, May, time = 1300 GMT

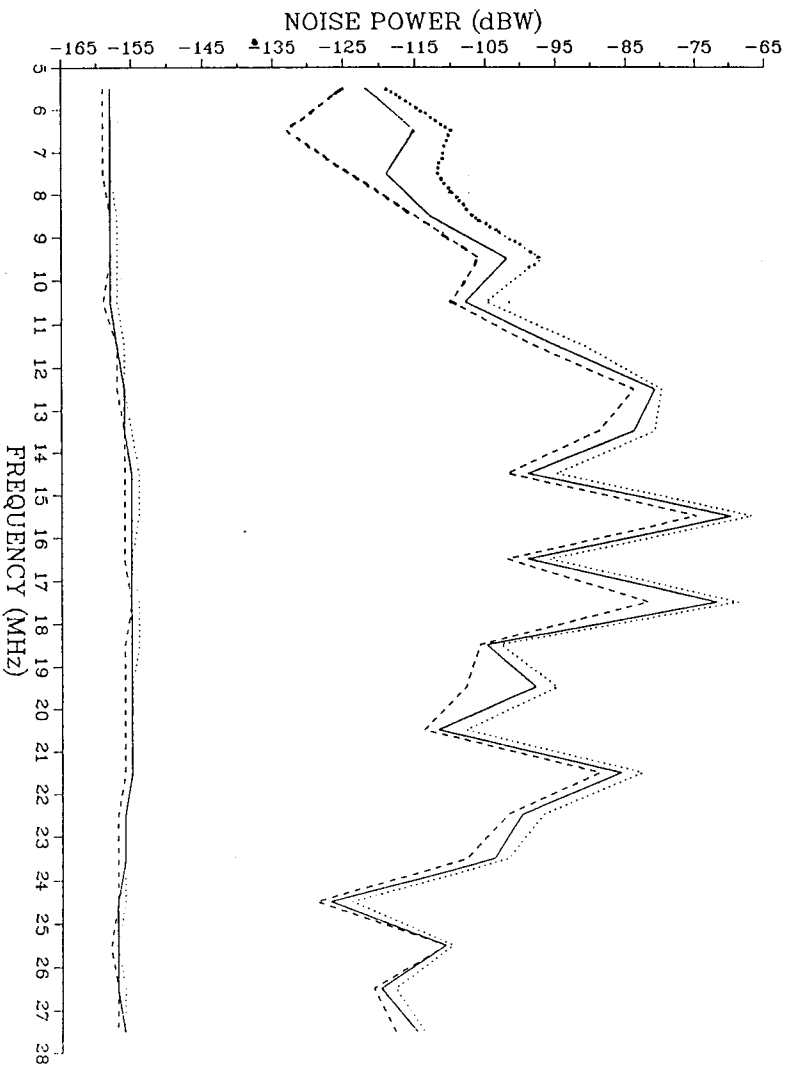
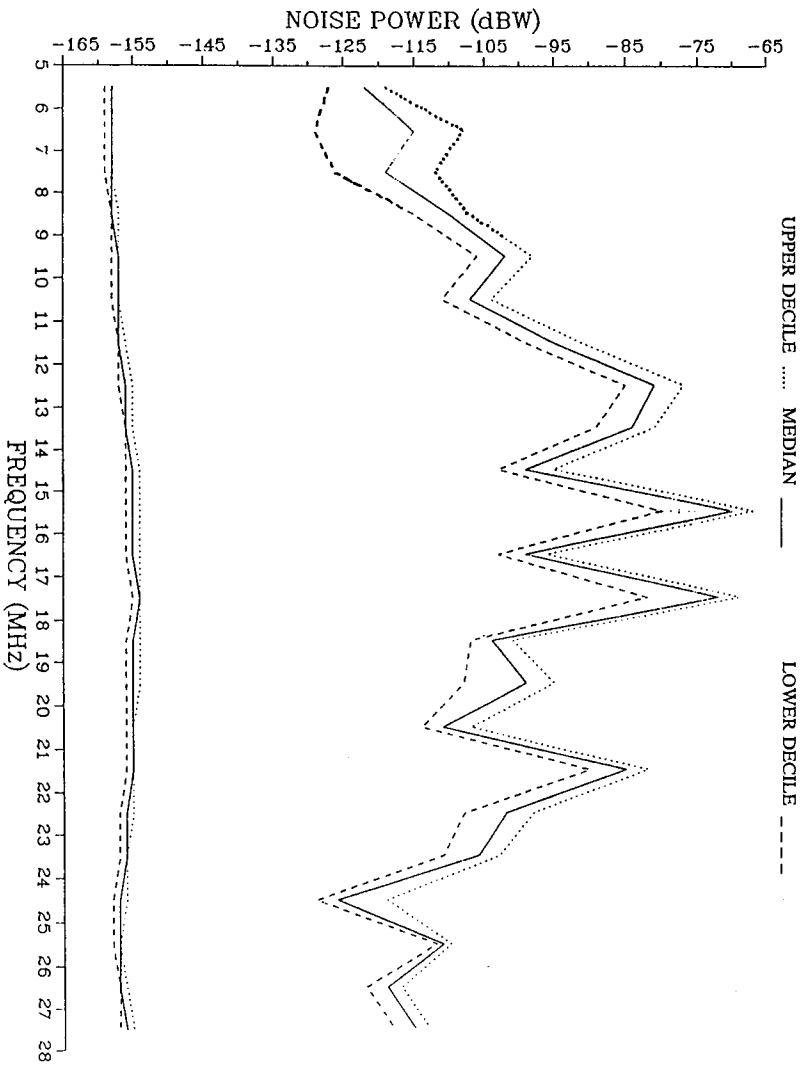


Fig. 7 — ROTHF signal and noise statistics, Amchika for (a) one hour, and (b) 30 min. time intervals

3. DISTRIBUTIONS OF SPECTRUM MONITOR DATA

Power levels indicated in the spectrum updates will be used to estimate channel availability and duration based on the statistics of the noise in each analysis interval. Knowledge of how these amplitudes are distributed with respect to time of day will assist in determining availability and duration of channels' at the ROTH Amchitka site. To understand the characteristics of the channel power levels, empirical distribution functions (EDFs) were generated based on 1 MHz analysis intervals in the frequency range from 5 MHz to 28 MHz during the time periods of 00Z and 12Z. To analyze the behavior of the power levels, a comparison of empirical cumulative distributions of channel amplitudes for 1 and 16 spectrum updates (25 s and 7 min, respectively) were generated from measurements of the HF spectrum during the months of January, April, July, and September at the Amchitka site. Figure 8 shows the EDFs that are representative of the behavior of the channel amplitudes when 1 and 16 update data sets were compared. Furthermore, the characteristics indicated by the EDFs support the findings noted in Section 2.1, i.e., that the power levels show amplitude stability over time. Therefore, based on the behavior of the data observed in the EDFs, it is reasonable to expect agreement between the MEOMIs, since their distributions are nearly coincident for two distinct intervals of time within a given time period.

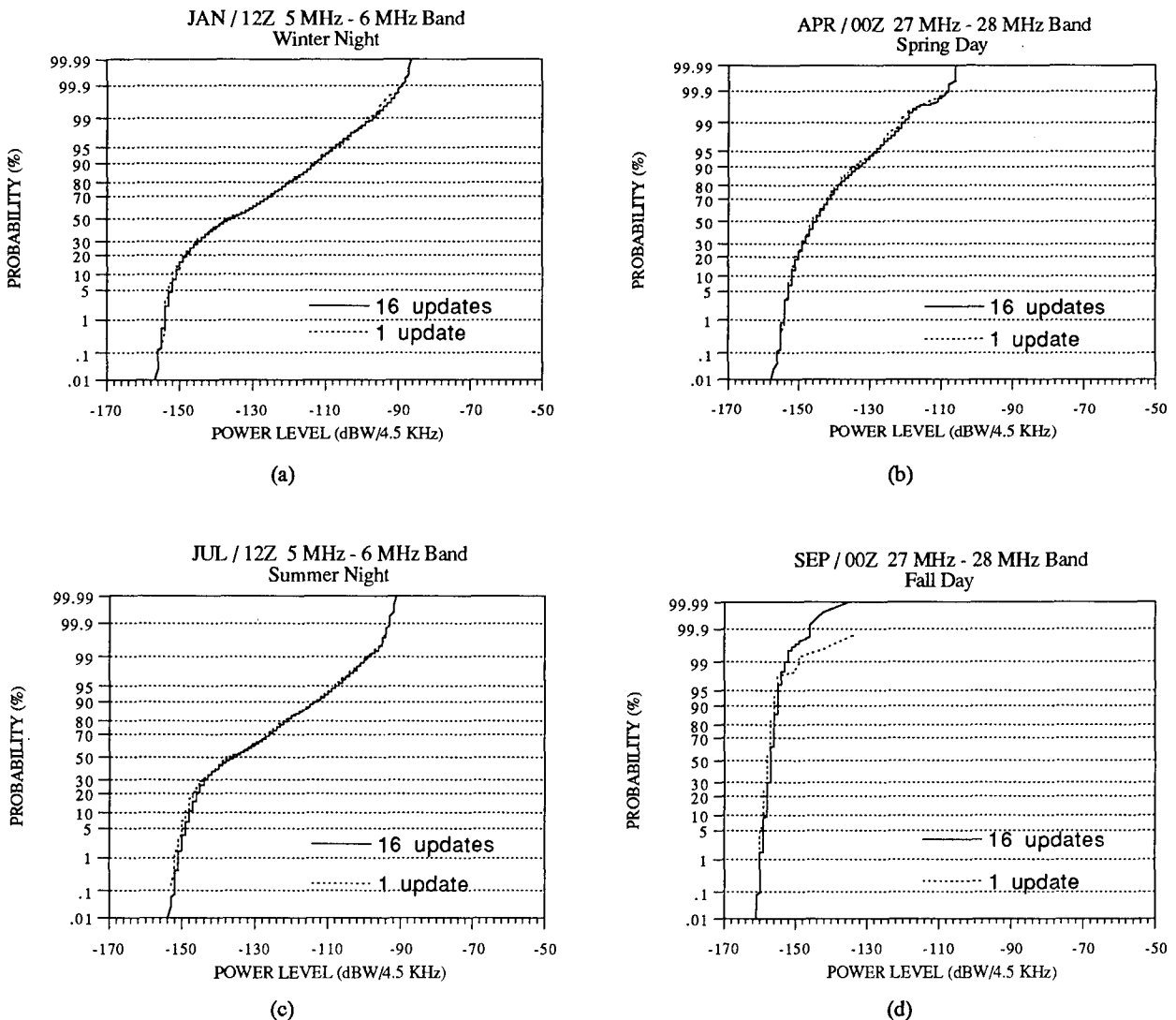


Fig. 8 — Examples of EDFs for 1 and 16 updates

The curves shown in Fig. 8 indicate no significant difference between the sample distribution for a single update (333 sample points) when compared to the distribution using 16 updates (6000 sample points). Thus, the distributions of power levels will be useful in setting thresholds for determining channel availability. Specifically, the EDFs indicate that the range of power levels is similar in magnitude as a function of frequency and time of day, and in particular the characteristics of noise-only channels, i.e., the channels with the lowest amplitudes are observed to have the same order of magnitude range regardless of season.

The curves shown in Fig. 9 are representative of the distributions of power levels observed during the time period of 12Z in the 27 MHz to 28 MHz frequency band for any given day of the months indicated. For the ROTH site in Amchitka, this is the time and frequency interval when a minimum of HF transmissions are expected to occur. Therefore, the EDF of the measured power levels during this time period and frequency interval should provide an indication of the power levels that are associated with atmospheric and galactic noise at the radar site.

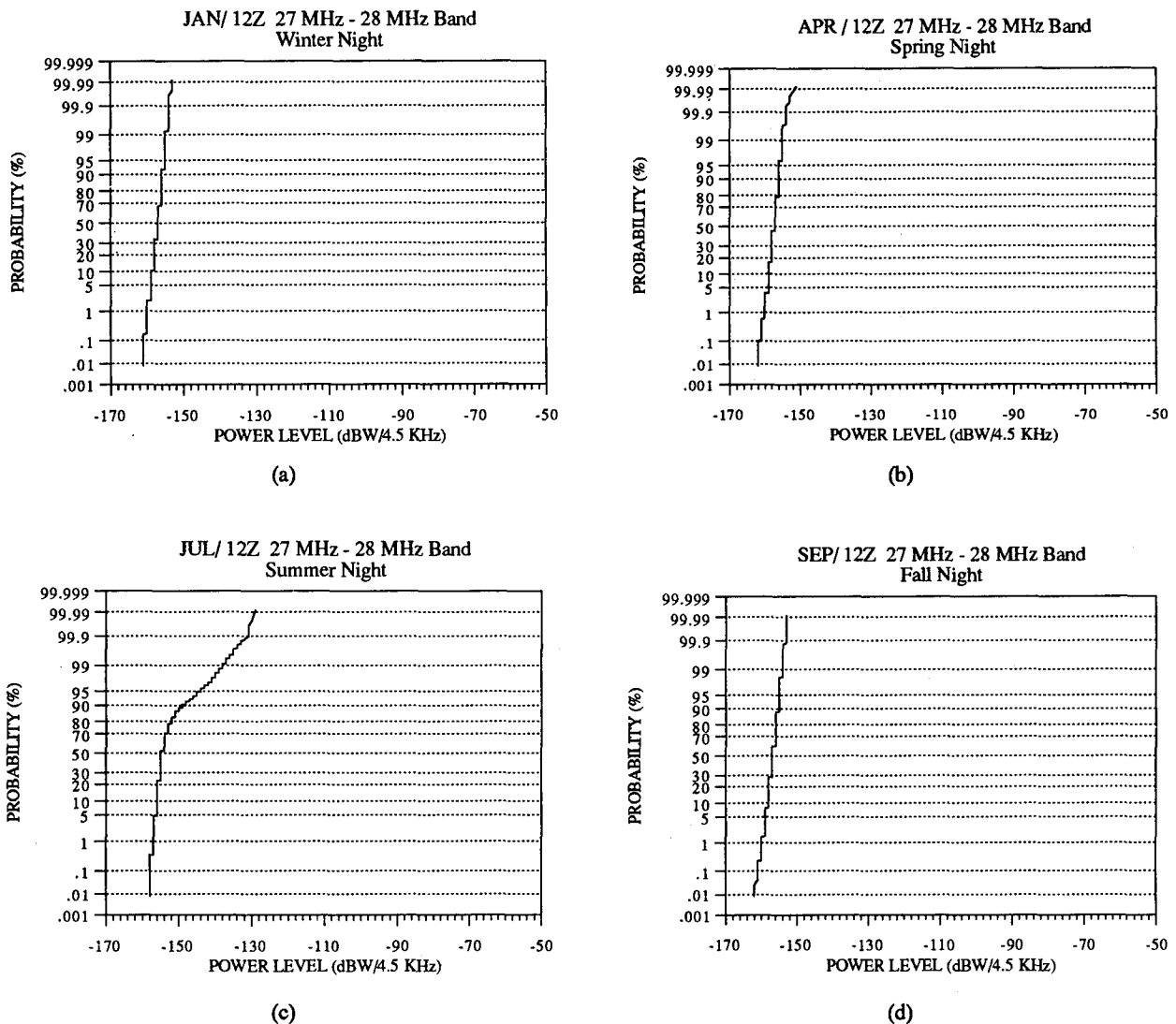


Fig. 9 — Examples of nighttime EDFs

An analysis of the EDFs represented in Fig. 9 indicates that channel power levels in this frequency band and time period were generally in the interval $(-163, -150)$ dBW, with July being the exception. Furthermore, the EDFs of the power levels are generally characterized by nearly vertical lines (steep positive slopes), which implies that small deviations in the amplitudes of the power levels occur during this time period and frequency interval. Generally, the density of the ionosphere at the radar site during this time period will not support skywave propagation in this frequency band. However, the wide sweep backscatter ionograms (WSBIs) of Fig. 10 indicate there was sporadic E transmission out to 28 MHz during July nighttime which may account for the high power levels in the summer night EDF. Therefore, for the Amchitka radar site, the measured power levels for nighttime in the 27 MHz to 28 MHz band will most likely represent local atmospheric and galactic noise, and will be unlikely to contain signal transmissions from any HF spectrum users. Therefore, the power amplitudes of channels representing local atmospheric and galactic noise will be defined by the power amplitudes indicated in the EDFs shown in Fig. 9. Thus, any channel with power levels in the $(-170, -150)$ dBW interval will be considered to represent environmental noise, and therefore may be tested for available use by the ROTHF (see Section 6).

To verify the results based on the analysis of the EDFs presented in Fig. 9, distributions of channel power levels were generated for times and frequency intervals where noise and HF users were expected to exist during radar operations at the ROTHF site. Figure 11 shows representative samples of these EDFs. A probability plot is used, as is the case of the other EDFs, to examine the peculiarities of the channel power levels noted above. Reference 6 provides a discussion and further references on statistical analysis based on empirical distribution functions. In particular we are interested in distinguishing power levels associated with noise and HF users, as opposed to general characteristics of channel amplitudes investigated in Figs. 8 and 9.

The distributions shown in Fig. 11 are the EDFs of the noise and HF users for the indicated periods, and are represented by curves with two distinct slopes. Therefore, consider truncating the curves above the 99% horizontal line, and drawing a vertical line from the intersection of the two slopes to the horizontal axis. For each of the seasons, the day and night curves are represented by two slopes (with the exception of January night, where only one slope is present), over the range of power levels indicated on the abscissa. In almost every instance, the power levels below the intersection of the two slopes are less than -150 dBW and have characteristics that were indicated by the distribution of noise-only channels. Thus, the aforementioned particularities are present in each of the plots, and power levels associated with this portion of distributions are defined over the -170 dBW to -150 dBW amplitude range. That is, the distribution of the power levels in this amplitude interval is shown to have small deviations, and is represented by a line segment with a steep positive slope. Specifically, these results indicate that channels with noise and HF traffic can be identified based on the channel power level measured by the ROTHF SM.

Employing the definition of noise, the following characteristics can be observed from the empirical distributions:

- (1) no apparent difference between one spectrum update (25 s) and that of 16 consecutive spectrum updates (7 min);
- (2) channels with only noise will generally have amplitudes between -170 and -150 dBW;
- (3) EDFs of analysis intervals with noise only are generally represented by a line segment with a steep positive slope over the amplitude range indicated above; and
- (4) EDFs of analysis intervals with noise and HF users present are generally represented by curves having two distinct slopes.

In addition to analyzing empirical cumulative distributions, probability mass functions (pmfs) were also investigated to determine if other characteristics of the channel power levels could be identified.

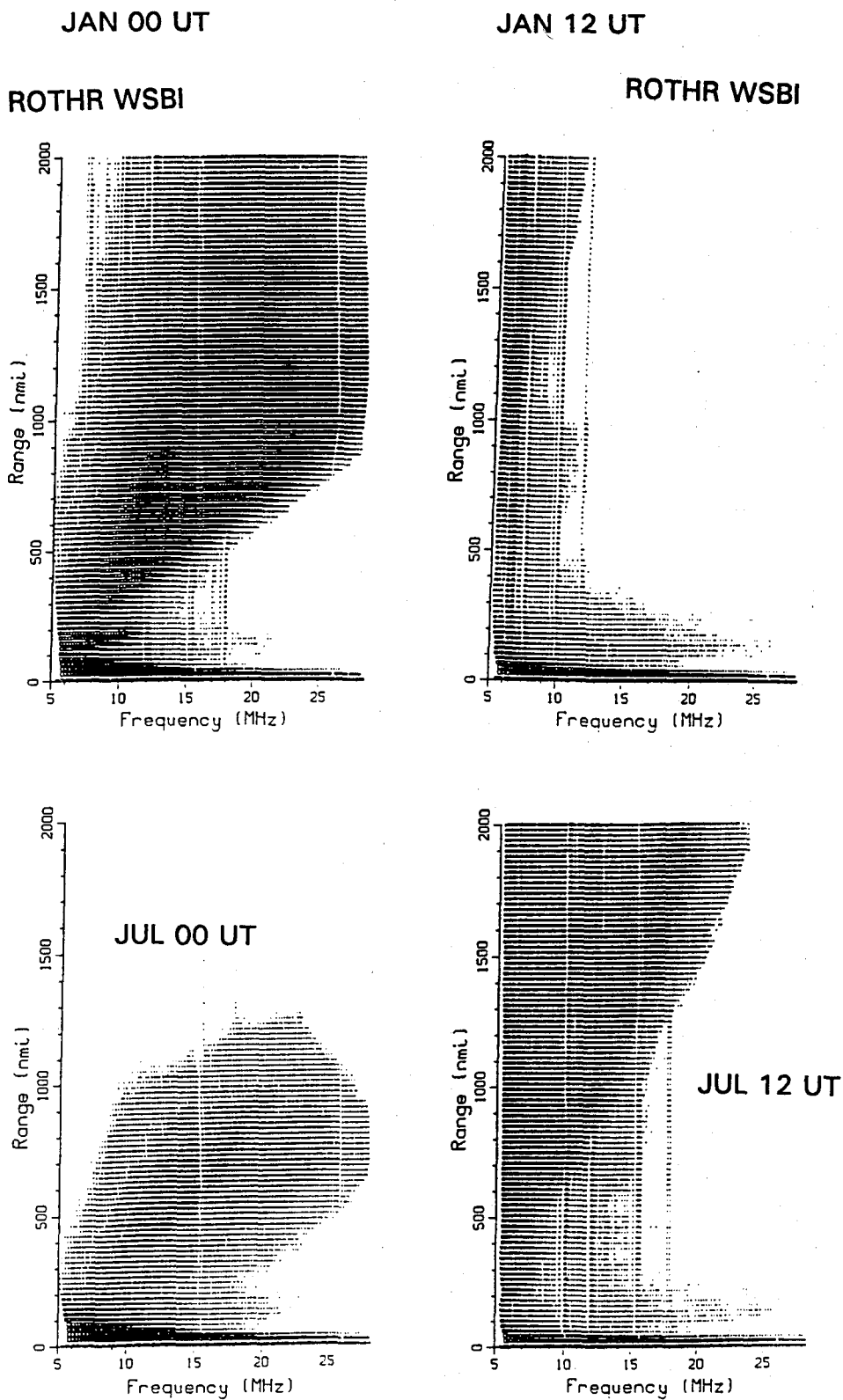


Fig. 10 — ROTHR wide sweep backscatter ionograms for winter and summer

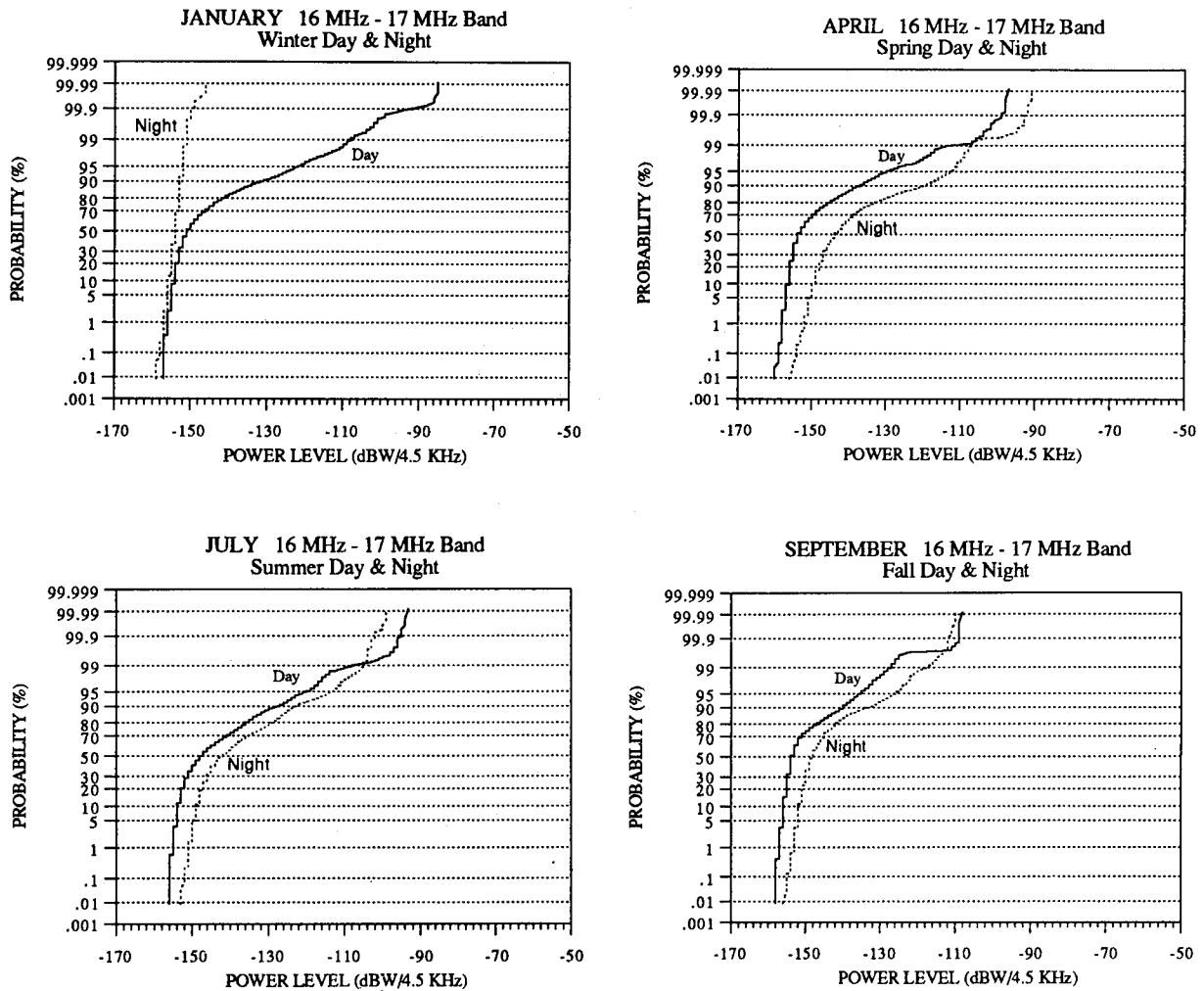


Fig. 11 — Examples of day and nighttime EDFs

Representative examples of the probability mass functions derived from the spectrum measurements during the indicated time and frequency interval are shown in Fig. 12. These graphs emphasize the characteristics noted in the pmfs for the time and frequency interval indicated. An examination of these frequency distributions will show characteristics in the data which indicate seasonal changes that are not as evident from the EDFs. Two of the most noticeable differences that were observed in the pmfs are indicated in the graphs in Fig. 12.

Results based on the analysis of empirical and frequency distributions have identified characteristics in the spectrum updates which appear to be a function of time, frequency, and season. These features can be used to identify power levels for establishing noise thresholds and other decision rules for defining channel availability and duration. Analysis of the data presented in this section indicates that two distinct curves are usually present in the empirical cumulative distributions, where the background noise is indicated by a vertical line having a steep positive slope, and the HF traffic (users) are represented by the line segment defined for amplitudes greater than -150 dBW. The pmfs provide additional information on HF traffic for a given time of day and season of the year, which can be observed in the upper tails of the frequency distributions. The high power levels indicated in the tails of the pmf are associated with the HF traffic.

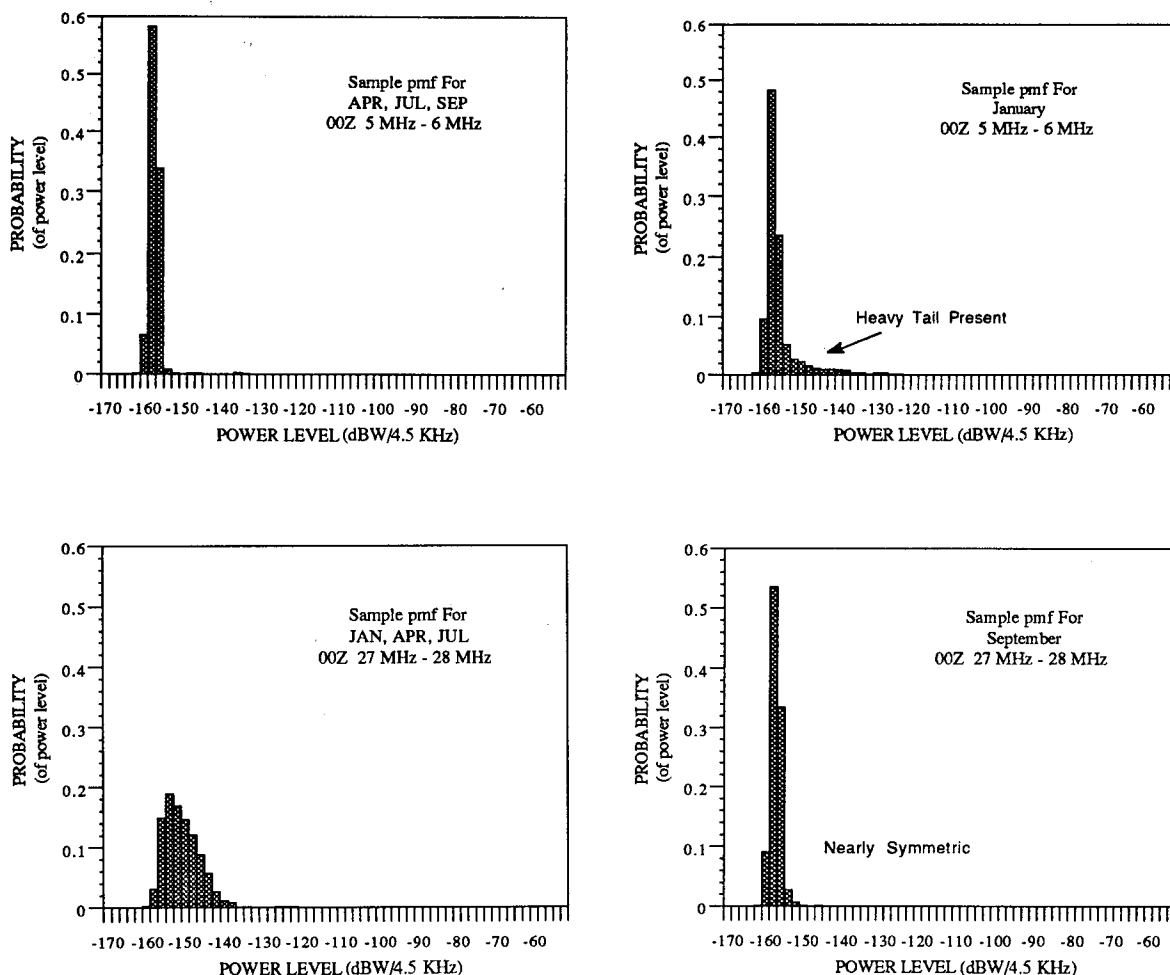


Fig. 12 — Examples of probability mass functions

4. SM NOISE MEASUREMENTS VS SPECIFICATION REFERENCE LEVEL

To determine if the ROTHr was externally noise limited, estimates of the noise floor, the MEOMIs, were obtained over 5 days during July and September, respectively, and compared to the radar's specification reference level (SRL). The SRL represents the smallest signal in a 1 Hz bandwidth that can be measured by the ROTHr SM receiver. This level is defined by

$$SRL (dB) = kTB (dB) + noise\ figure\ of\ receiver (dB) = -204\ dB + 14.5\ dB = -189.5\ dB.$$

The difference between the estimates of the noise floor and the SRL were used to determine when the ROTHr was externally noise limited during the months of July and September. Before this difference could be obtained, the noise estimates were converted to an equivalent noise level (ENL) in a 1 Hz bandwidth. Since 4.5 KHz (the SM noise bandwidth) is equivalent to $10(\text{Log}_{10}(4500)) = 36.5$ (dB), the ENL in a 1 Hz bandwidth is obtained by adding -36.5 dB to the MEOMI. A comparison between the noise estimates and the SRL can be made by subtracting the ENL from the SRL which results in a noise delta for each analysis interval. If the noise delta is equal to or greater than zero, the indication is that the radar was externally noise limited during that time period and frequency interval.

A comparison between the analyzed SM data and SRL are shown in Figs. 13 and 14 for a typical day during the months of July and September, respectively. The analysis indicates that for July, the measured noise exceeded internal noise from 8 to 16 GMT and for frequencies between 5 MHz and 17 MHz. Results shown in Fig. 14 (September data), indicate that the noise deltas are greater than zero from 8 to 16 GMT and for frequencies from 5 MHz to 15 MHz. Specifically, ROTHF Amchitka appears to be externally noise limited between these hours and frequencies for the months indicated.

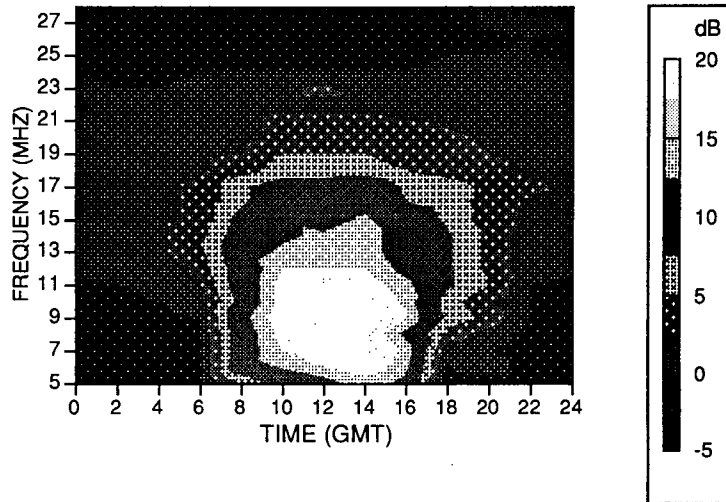


Fig. 13 — July radar noise vs specification level (-189.5 dBW)

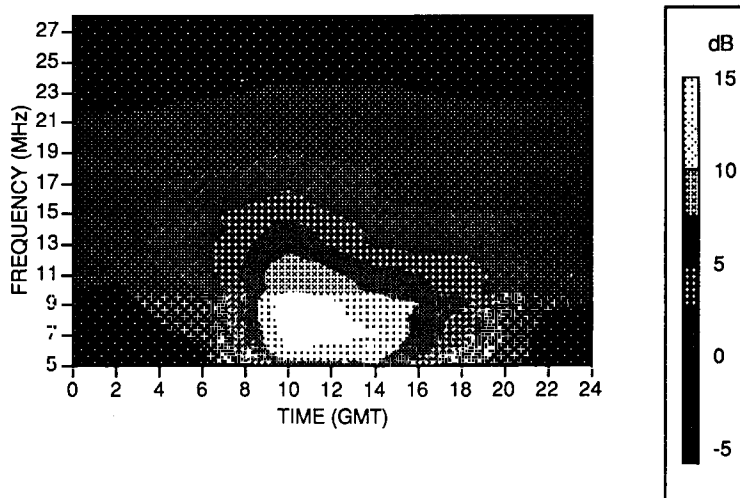


Fig. 14 — September radar noise vs specification level (-189.5 dBW)

Seasonal comparisons of the noise deltas are shown in Figs. 15 and 16. Based on the data presented in these figures, the ROTHF appears to have been externally noise limited for both day and night cases, even though the differences between the noise estimate and the reference level are in some cases less than zero. However, observing that the difference is changing as a function of frequency, a characteristic of external noise and not internal noise, indicates that the ROTHF was externally noise limited during these time periods.

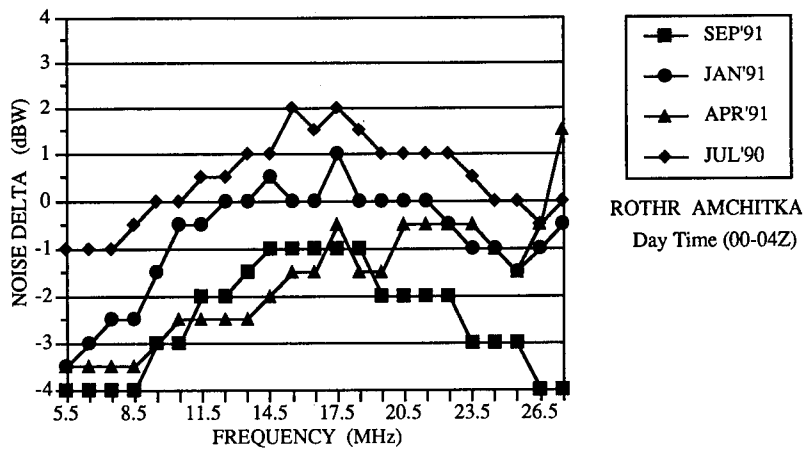


Fig. 15 — Radar noise vs specification level (-189.5 dBW), daytime (00-04Z)

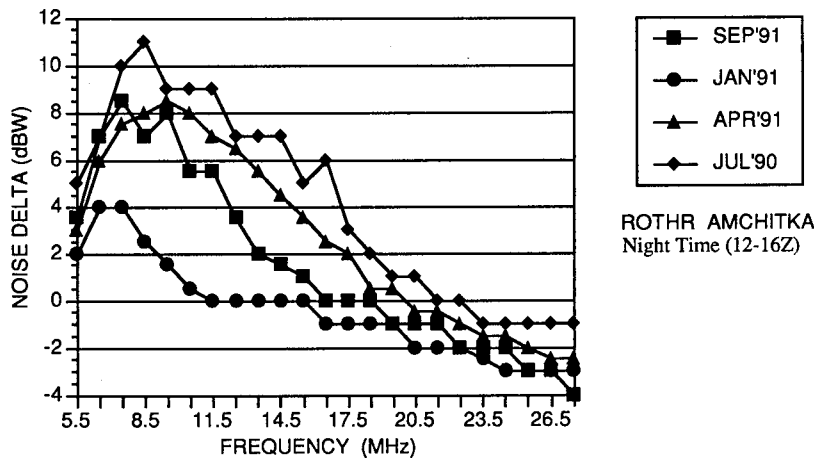


Fig. 16 — Radar noise vs specification level (-189.5 dBW), nighttime (12-16Z)

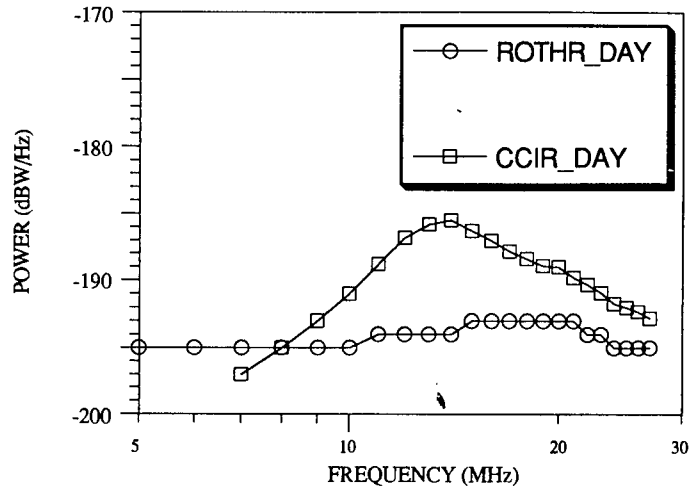
5. SM MEASUREMENTS VS CCIR NOISE PREDICTIONS

In this section, noise estimates derived from Amchitka SM data are compared with the CCIR 322 [3] noise predictions for day and nighttime ROTH operations, and the results are shown in Fig. 17. In order to compare these data sets, adjustments were made to both. First, the noise estimates were converted to ENLs in a 1 Hz bandwidth, and second, the losses of the SM's receive antenna were added to the CCIR predictions.

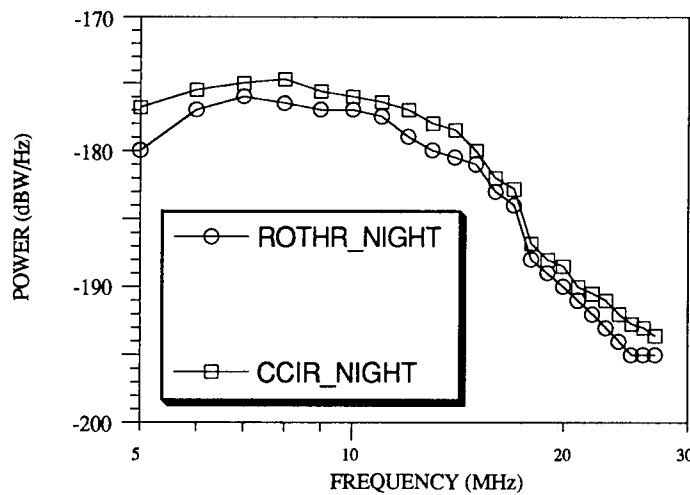
The data presented in Fig. 17 represent July daytime and nighttime, (00Z to 04Z) and (12Z to 16Z), respectively. The CCIR curve represents the combined atmospheric and galactic noise predictions, and the ROTH curve represents the MEOMI derived from the data sets sampled during the indicated time periods. It appears that the ROTH noise estimates are influenced primarily by the predicted galactic and atmospheric noise curves during the nighttime hours, and are relatively flat with respect to frequency during the daytime hours. The agreement between the two data sets appears to be best during the nighttime hours.

5.1 SM Noise vs Radar Log-Amp Noise

ROTHR log-amplitude (log-amp) data is another source of noise estimates. Noise measurements from the log-amp data represent power levels based on active returns of the radar, whereas power levels based



(a)



(b)

Fig. 17 — ROTH SM estimates vs CCIR noise predictions
for (a) July 00Z and (b) July 12Z

on SM measurements are obtained from the passive subsystem of the radar. However, if Doppler regions are selected where no radar echoes exist, the log-amp radar data provides a measure of the noise. The power levels from the log-amp data are obtained from the range-Doppler-azimuth cells, which provide an indication of the noise level in a 1 Hz bandwidth of the radar's receive beam at plus or minus half the waveform repetition frequency (\pm WRF/2). If the noise levels from the two sources are different, this difference is an indication of how directional the noise is at the radar site. It is assumed that there is no self or active noise in the log-amp data, and therefore any characteristics of the noise between the two data sets which are significantly different would be manifested in the distributions of the power levels.

Empirical distributions were generated to investigate the differences between the noise levels from the log-amp and SM measurements. Figure 18 compares these noise distributions. January was the only month for which this analysis was performed, and the information presented in these plots is representative of the data analyzed. In comparing the distributions, the following parameters of the log-amp data were fixed: time, frequency, azimuth, and range. That is, to generate a time history of radar returns at \pm WRF/2, all returns within a 100 nmi range interval were combined, provided the returns were at the same operating frequency of the radar, azimuth angle off boresight, and in a fixed 10 minute

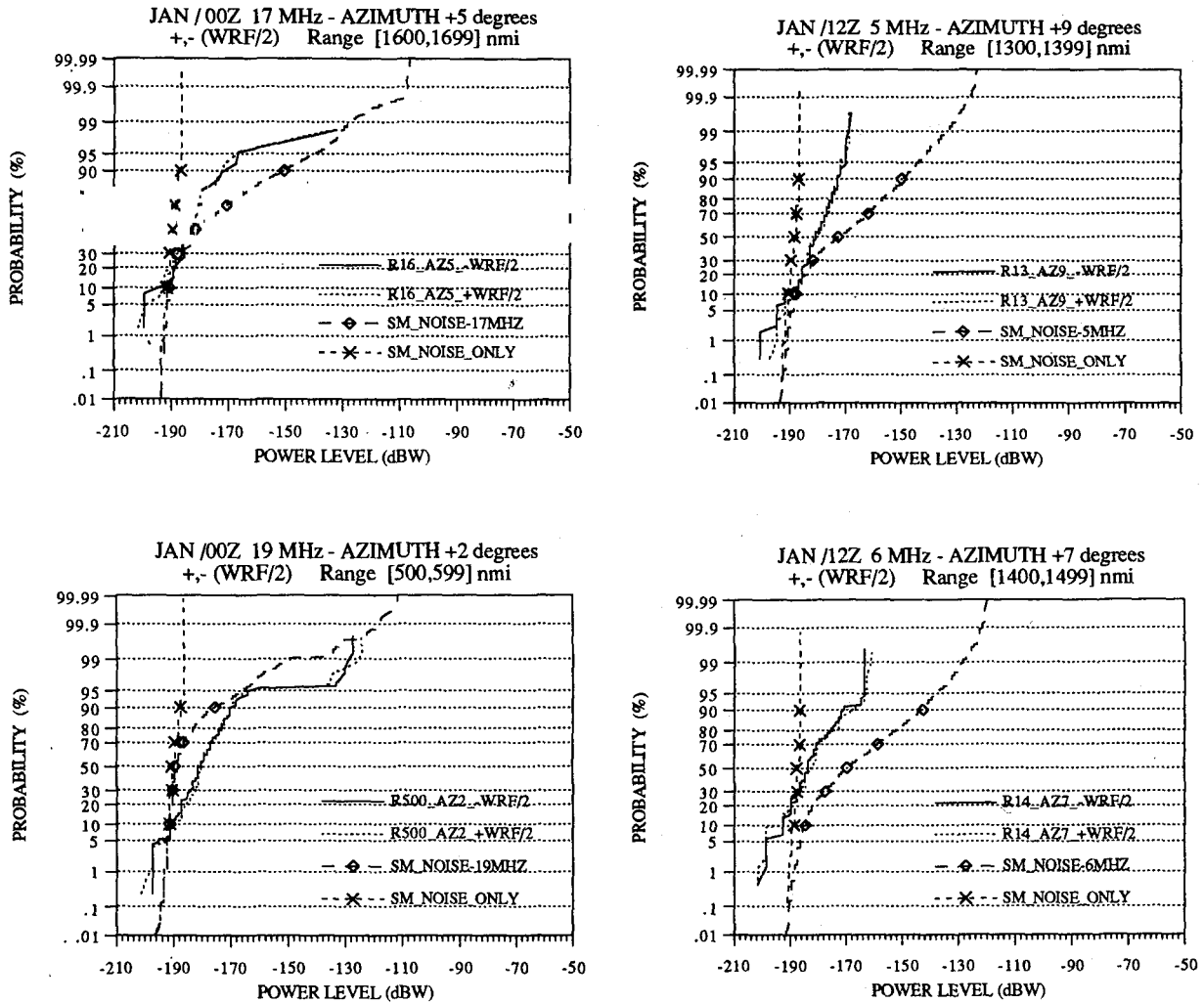


Fig. 18 — Log-amp noise levels vs SM noise levels

interval. These restrictions were in place because the log-amp radar returns are associated with different regions within the radar’s coverage area, which may have different revisit rates depending upon the region’s surveillance priority. To generate the sample distribution of log-amp data, the following requirements were considered for the January 5, 1990 radar returns:

- measurements between 00:10Z and 00:20Z,
- an operating frequency of 17.5 MHz,
- coverage area between 600 and 699 nmi,
- azimuth of +10 degrees from boresight.

Radar returns with these features would be processed from the log-amp data and used to generate the empirical distribution of the power levels with these parameters. This distribution is now compared to the EDF obtained from the SM measurements for the same month, day, 10 min. period, and MHz analysis interval. In general, the SM EDFs will contain a greater number of samples than the EDF of the log-amp data. However, combining the log-amp data as indicated provides ample data points with which to compare the EDFs.

For the plots shown in Fig. 18, the following format holds; the captions indicate the month, hour, and frequency interval in which the ROTHM was operating, the degrees off boresight, location of the

noise measurements (\pm WRF/2), and the range cells within the coverage area. The four curves represent the distributions of the measured active and measured passive power levels. The distributions representing the passive are labeled SM_Noise_xMHz and SM_Noise_Only, and are, respectively, the power levels measured by the SM and observed power levels in an analysis interval with only noise present. The distributions labeled Ryy_AZk_ \pm WRF/2 are the noise levels obtained from the log-amp data.

In each of the plots shown in Fig. 18, the following observations are evident; (1) noise levels at \pm WRF/2 are in excellent agreement with each other, (2) all distributions appear to be in agreement below the 30th percentile range, (3) the distribution of the log-amp data follows the distribution of power levels based on the SM data, and (4) these observations are true for each of the cases considered. The data imply no significant directionality in the noise environment at the Amchitka radar site.

6. DETERMINING CHANNEL AVAILABILITY

The analysis of channel availability and duration is based on using the first order statistic of the power levels in each MHz analysis interval. This statistic is used to define a threshold for channel availability with respect to each MHz interval in the HF spectrum. The threshold level for any analysis interval is defined to be 5 dB above the minimum signal level for that given band of frequencies. Specifically, we are allowing a channel's power level to be at most three times the power level of the smallest signal before declaring a channel occupied. Therefore, a criterion based on the minimum signal level plus 5 dB is used to identify available channels. This criterion was applied to spectrum measurements for the day and nighttime cases for the months of January, April, July, and September, which represented the measurements of the current ROTHF (Amchitka) HF spectrum database.

An update from the SM provides 7667 channels representing the frequencies between 5 and 28 MHz in 3 KHz steps. Of these channels, approximately half are restricted and not available for use by the radar. Since the operation of the ROTHF must not interfere with other users in the HF spectrum, a procedure that identifies channels in use would also indicate which channels in the spectrum are available. The procedure implemented to determine channel availability is based on the above threshold test. Figure 19 shows the possible locations of available channels in the HF spectrum based on a threshold test procedure.

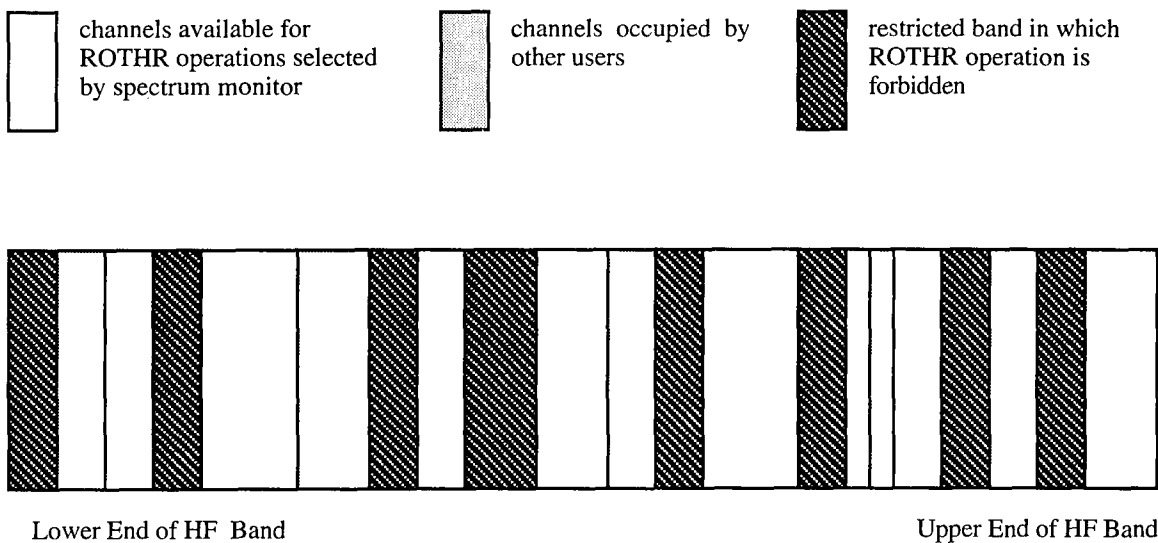
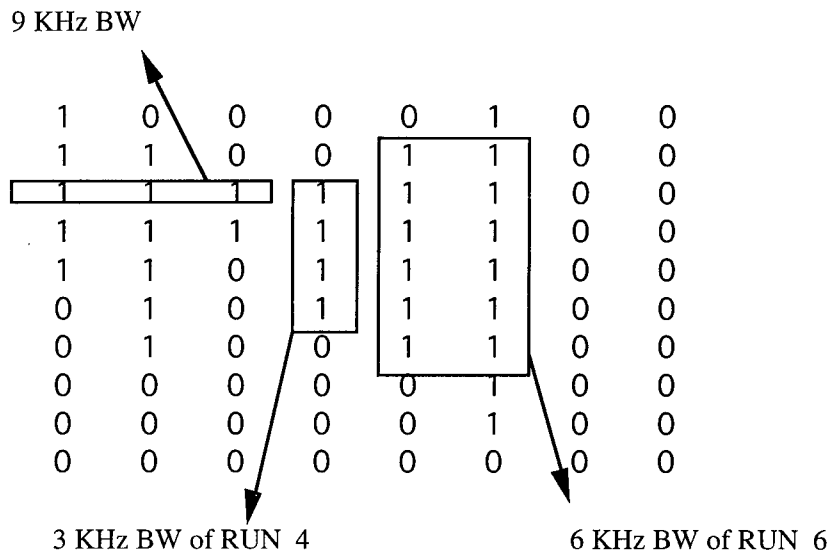


Fig. 19 — Selection of available frequencies for ROTHF

The duration (run) of a channel width is defined by the number of consecutive 1's appearing in the appropriate column(s). Channel width runs that would result from the processed data array in Table 2 are as follows. A channel of width 3 KHz would have runs of 5, 6, 2, 4, and 9, as indicated by the total count of consecutive 1's in columns 1 to 8. Note, columns that contain a repeat count, as illustrated by the count of 1's in columns 2 and 5, are only counted once. The duration of 6 KHz channels as indicated by the count of pairwise columns would have runs of 4, 2, and 6 resulting from the count of 1's in columns (1,2), (3,4), and (5,6), respectively. The duration of a 9 KHz channel would have runs of 2 and 4 as indicated by the count of triplets in columns (1,2,3) and (4,5,6), respectively. Likewise the duration of the 12 KHz, 15 KHz, and 18 KHz would all have a run of 2. Table 3 contains three examples of the various counts that were just described for available bandwidth and duration. Note, BW in Table 3 means bandwidth (i.e., channel width).

Table 3 — Examples of Duration Counts from Processed Data Array



7.1 Channel Availability Based On Decision Rule

The availability analysis was performed for day and nighttime periods for two consecutive days in each of the seasons. However, only one day for each season is shown to illustrate the observed characteristics. Results of the analysis are presented in the form of box plots [7] for selected channel widths. These plots show the availability characteristics with respect to the time of day and season of year. Because of the large number of channel widths that may be used by the radar, three representative channel widths were chosen to illustrate the availability characteristics. Widths of 3 KHz, 9 KHz, and 21 KHz were selected and the availability of these channel widths for day and nighttime usage in each season is presented in Figs. 20 through 27. In each display, general characteristics of the available bandwidths are indicated in each analysis interval. The horizontal axis is divided into segments of 5 MHz to 16 MHz, and 17 MHz to 27 MHz, and the vertical axis indicates the availability count, i.e., the number of times a channel of an indicated width was declared clear in the analysis interval.

With respect to channel width, time of day, and month, a rectangle is shown for each analysis interval indicating the following: the upper edge represents the third quartile for that channel width, the lower edge represents the first quartile for that channel width, the horizontal line inside the rectangle indicates the median availability count, the end point of the line from the upper edge indicates the largest count, the end point of the line from the bottom edge indicates the smallest count, and the circles above and/or below the largest or smallest availability count indicate possible outliers [5].

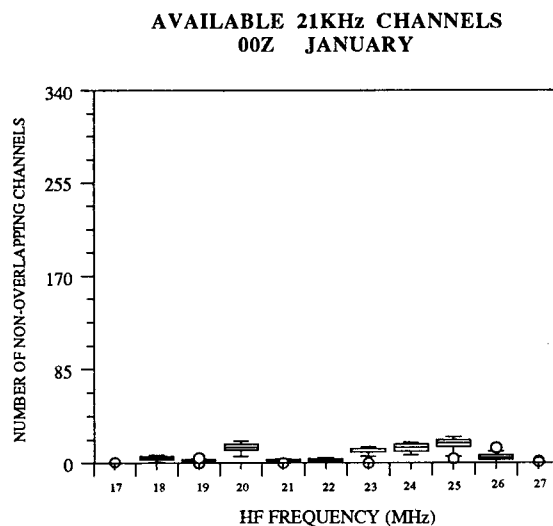
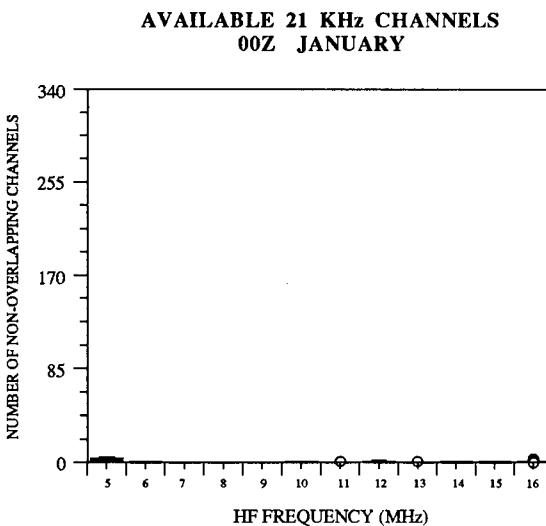
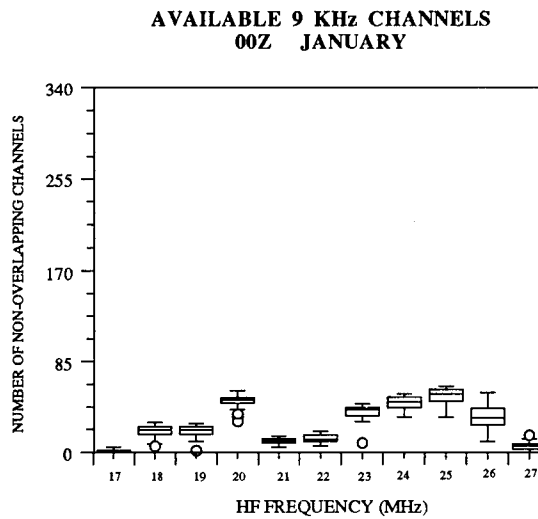
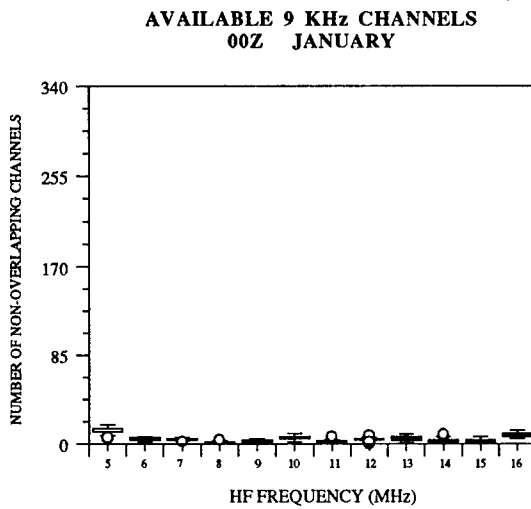
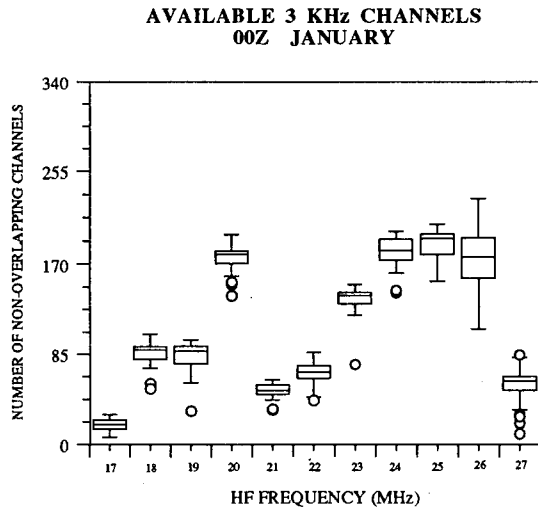
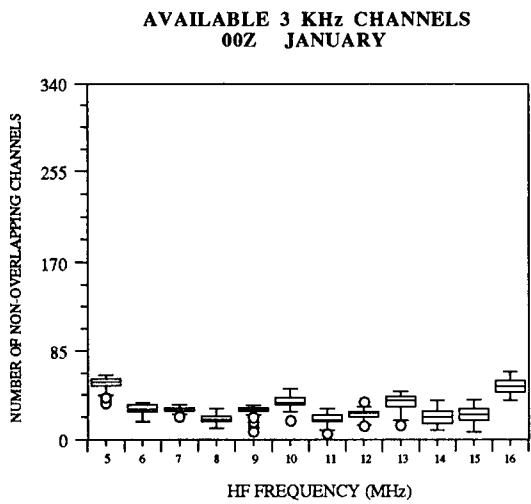


Fig. 20 — Channel Availability/January Day

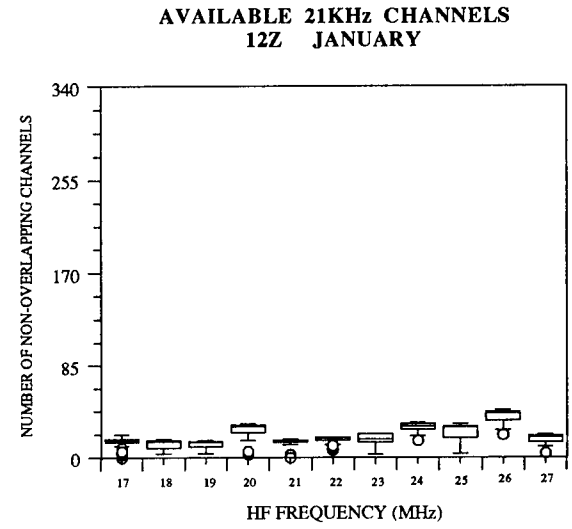
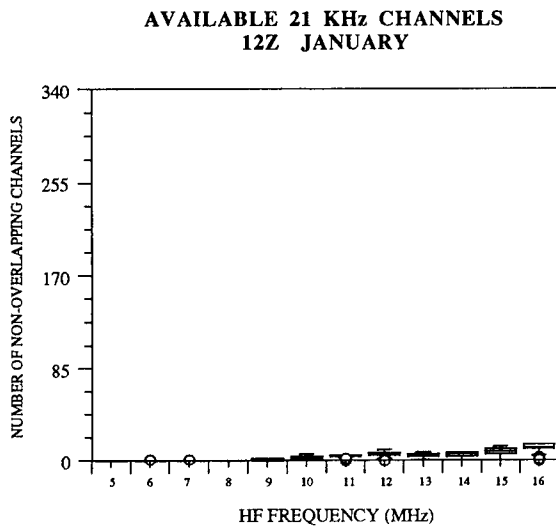
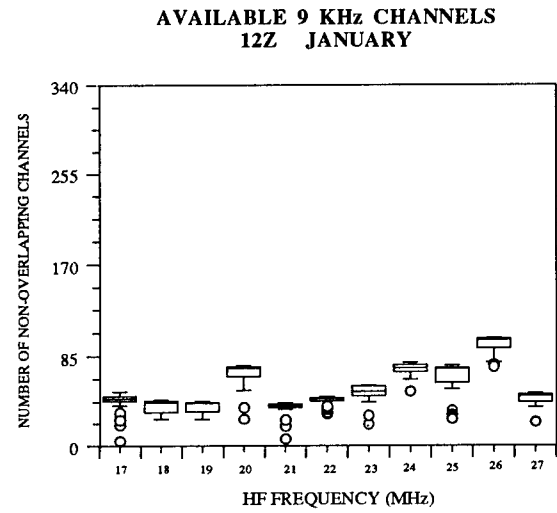
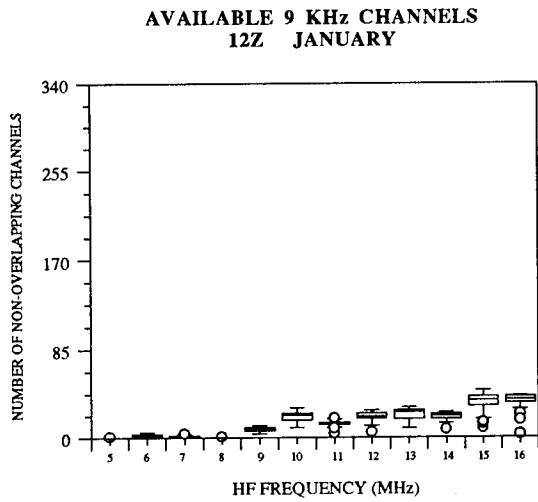
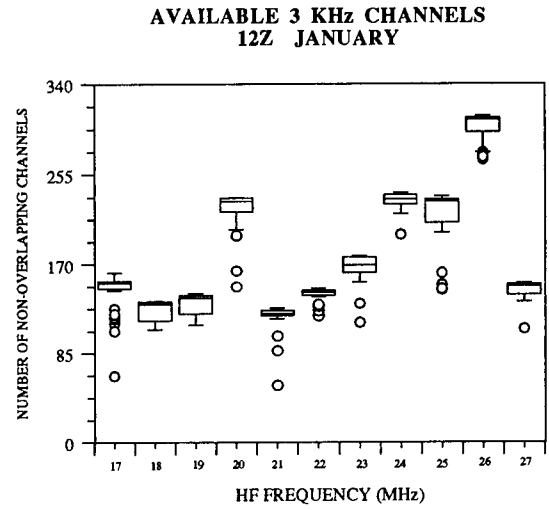
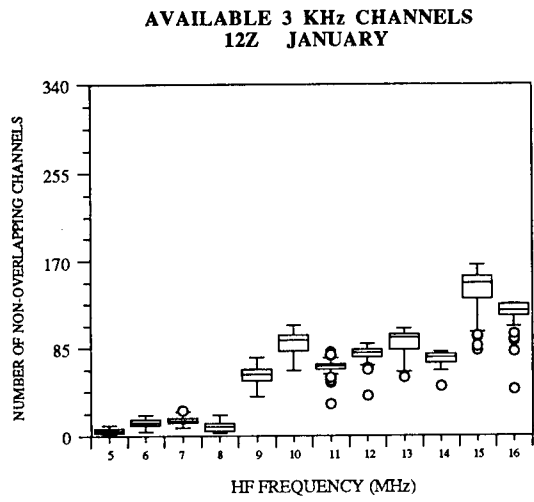


Fig. 21 — Channel Availability/January Night

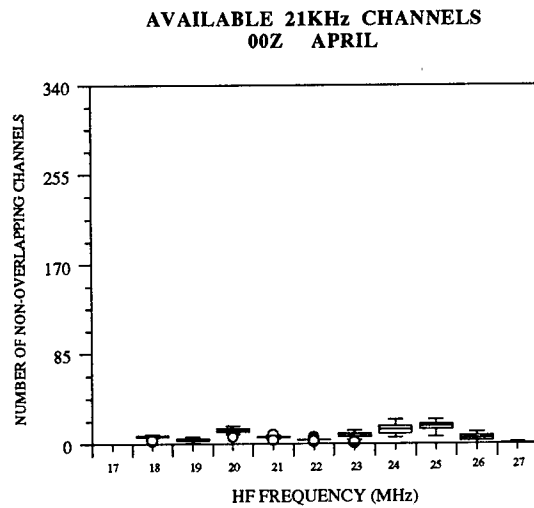
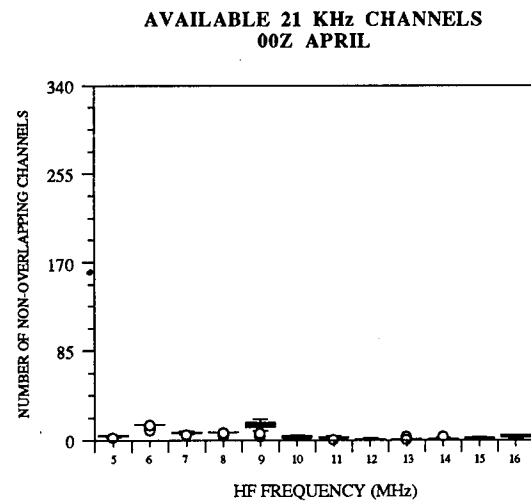
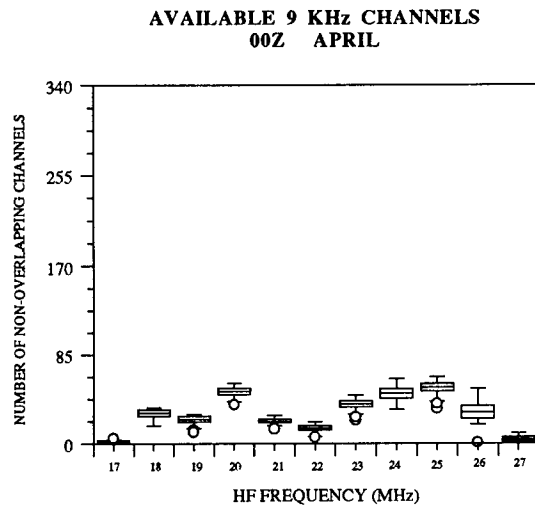
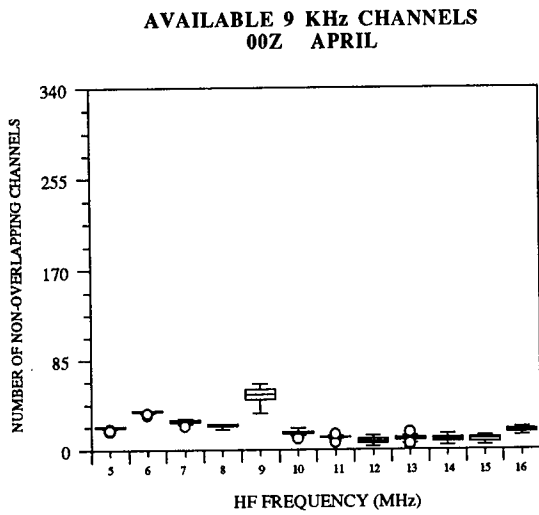
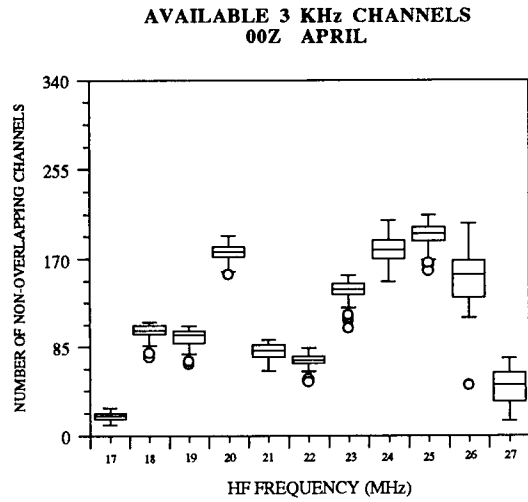
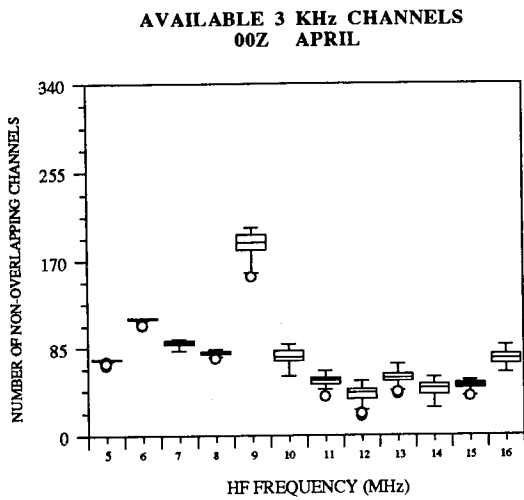


Fig. 22 — Channel Availability/April Day

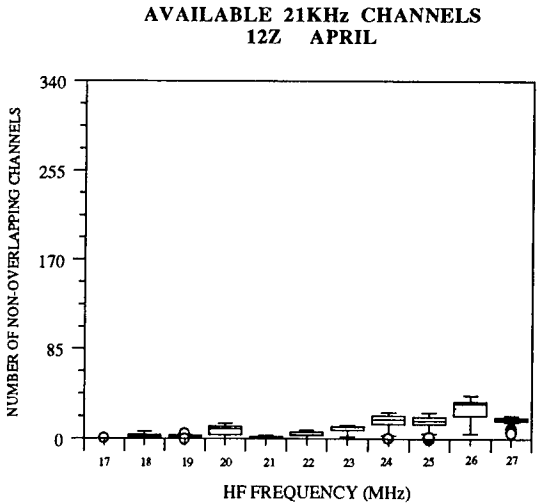
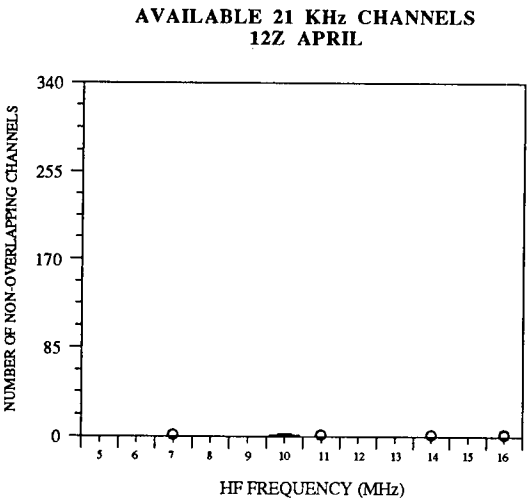
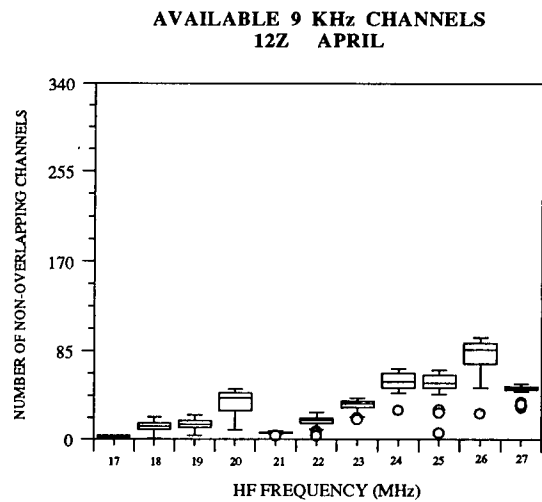
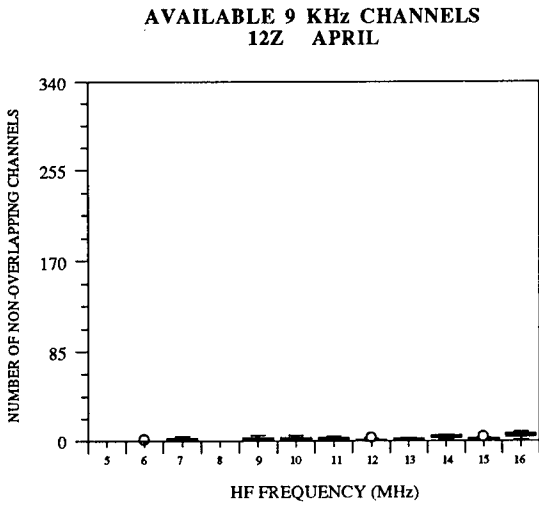
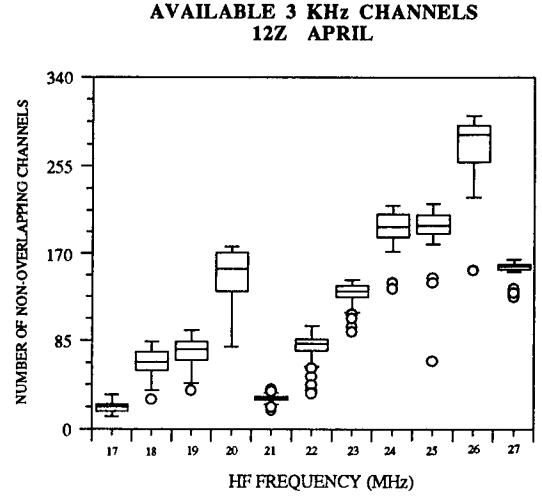
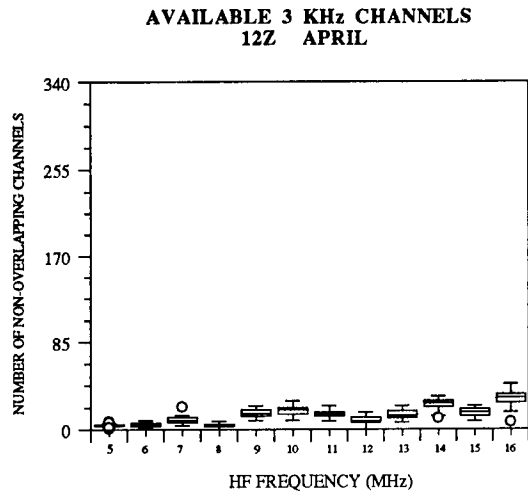


Fig. 23 — Channel Availability/April Night

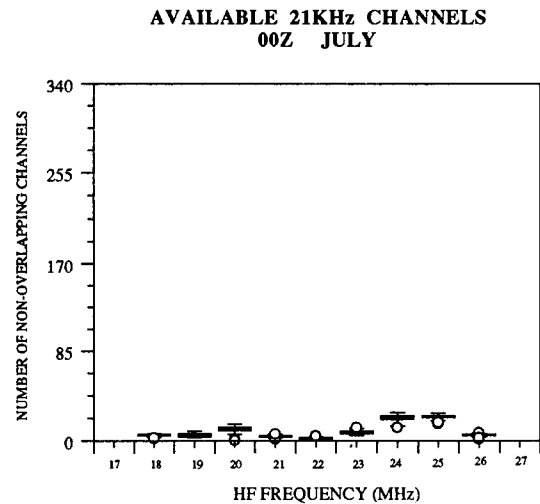
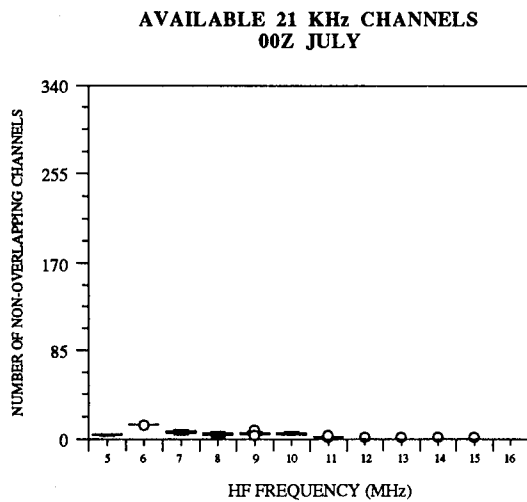
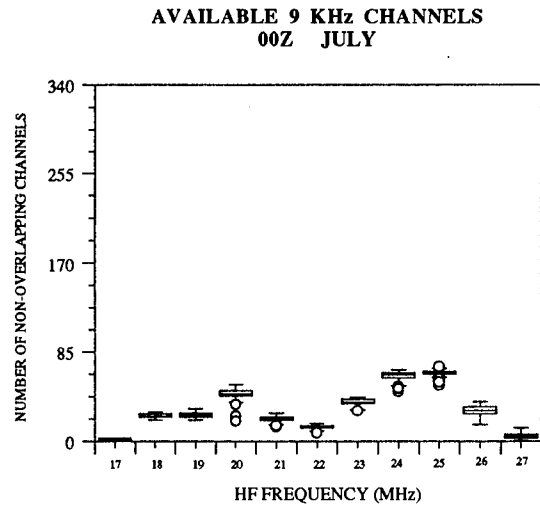
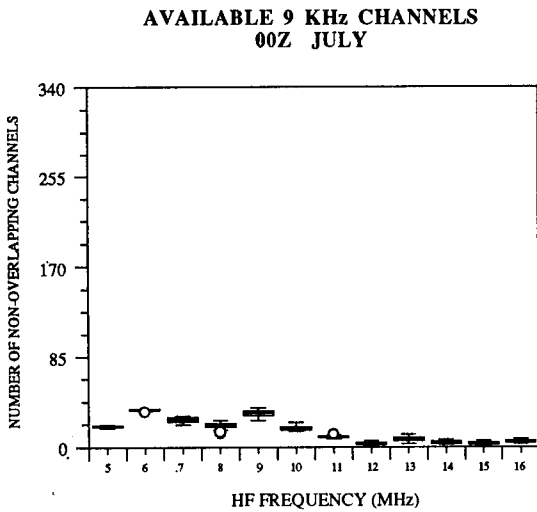
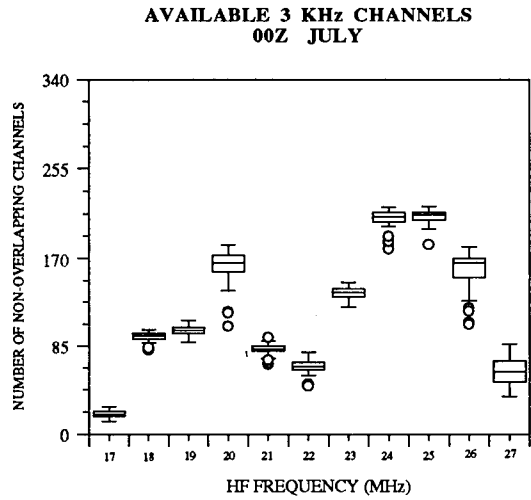
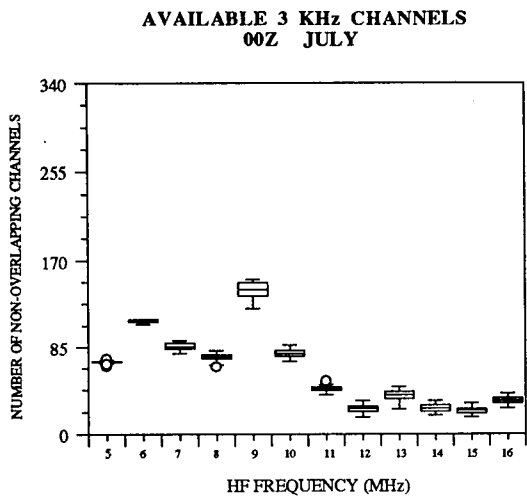


Fig. 24 — Channel Availability/July Day

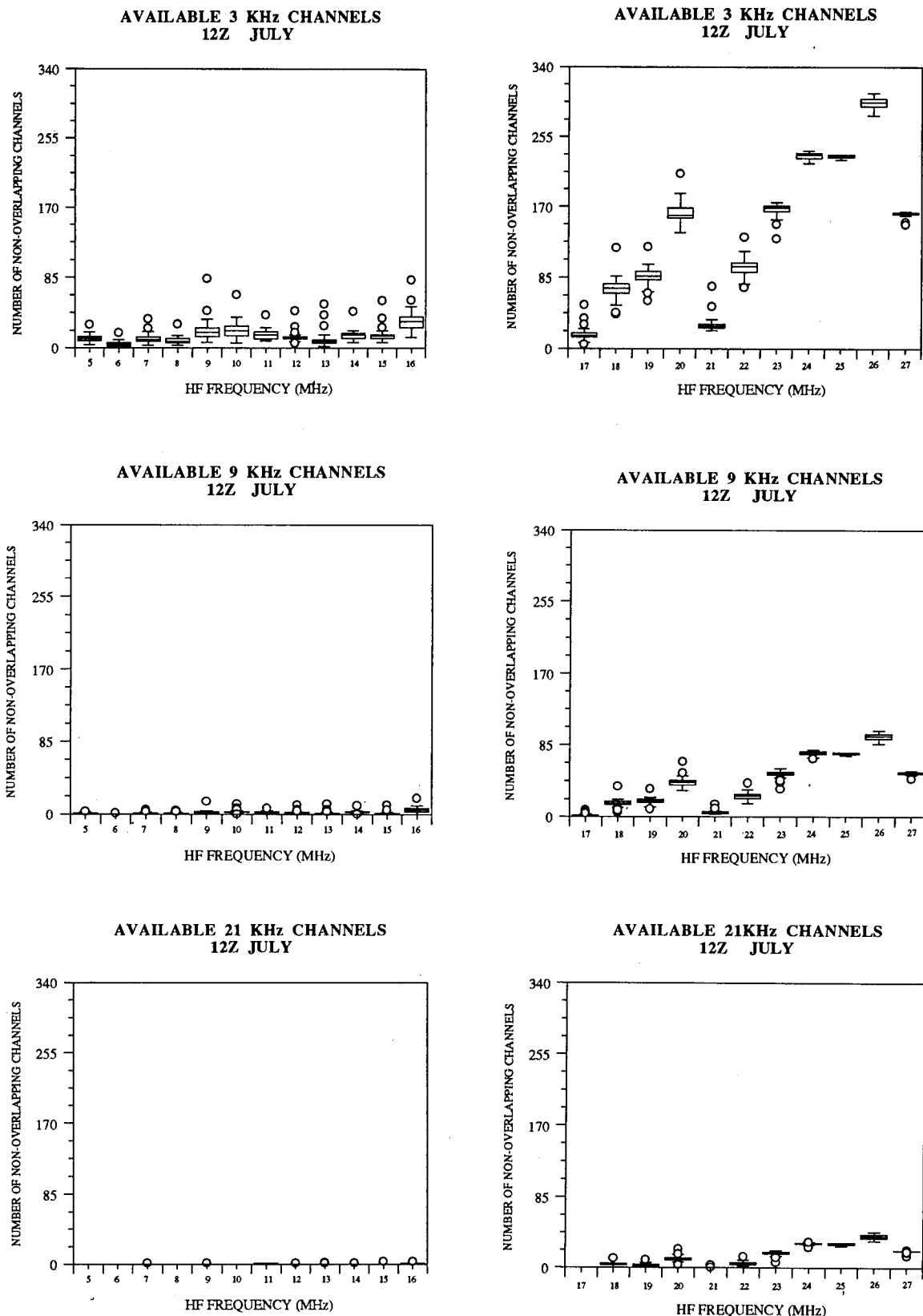


Fig. 25 — Channel Availability/July Night

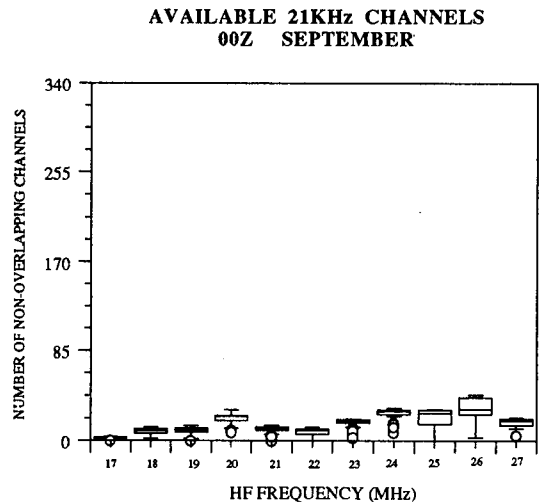
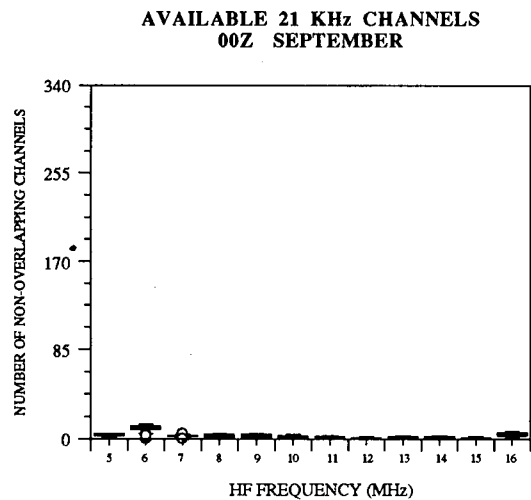
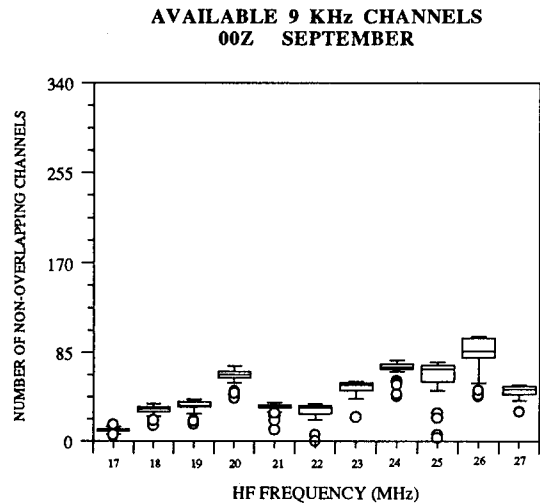
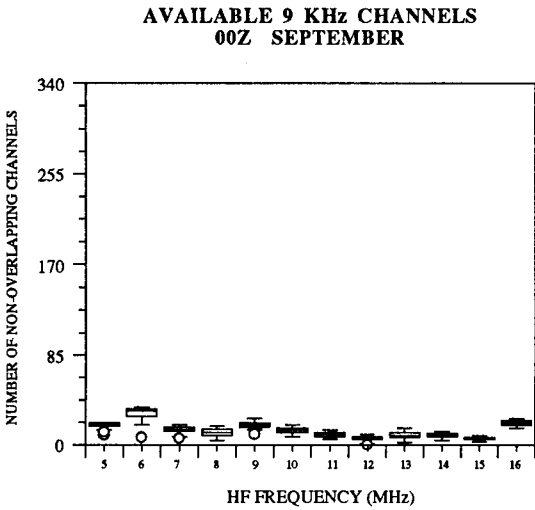
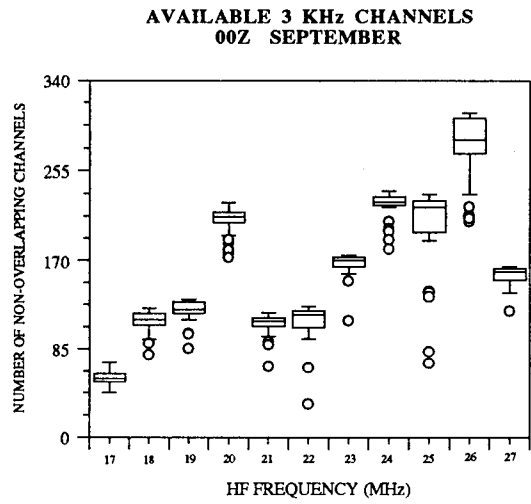
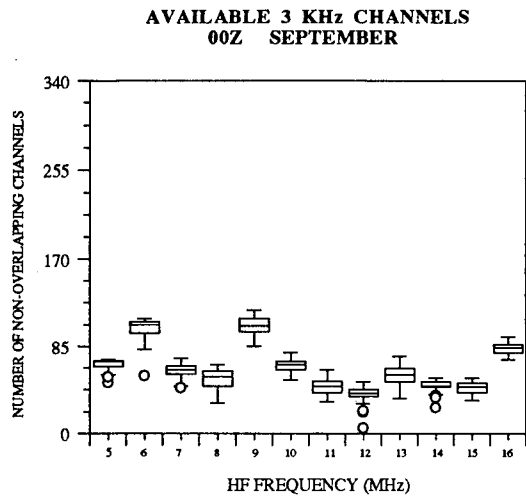


Fig. 26 — Channel Availability/September Day

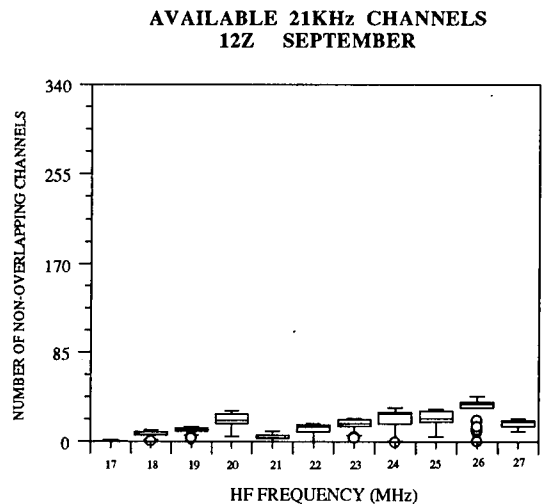
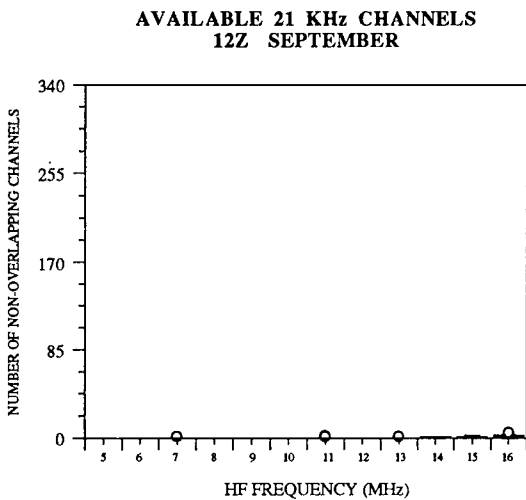
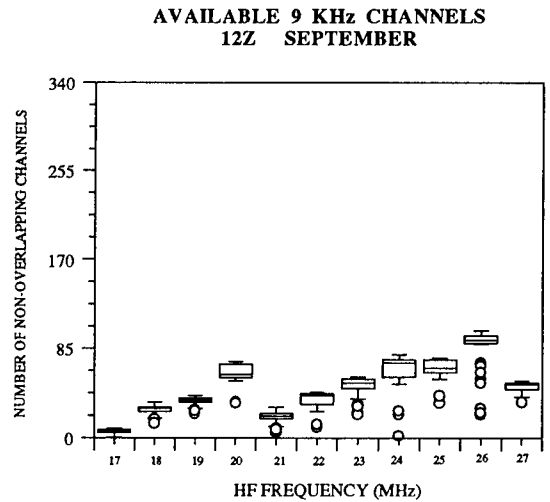
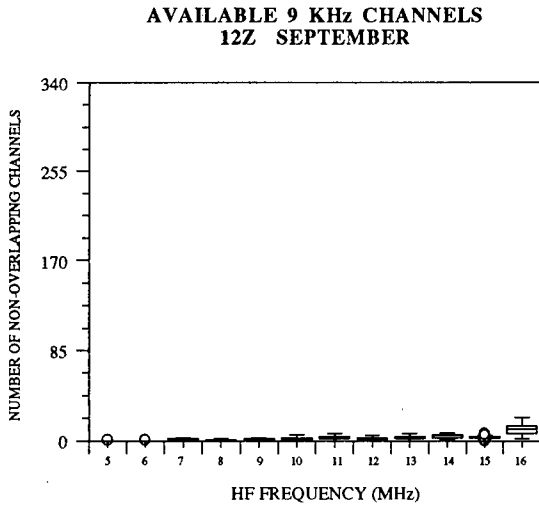
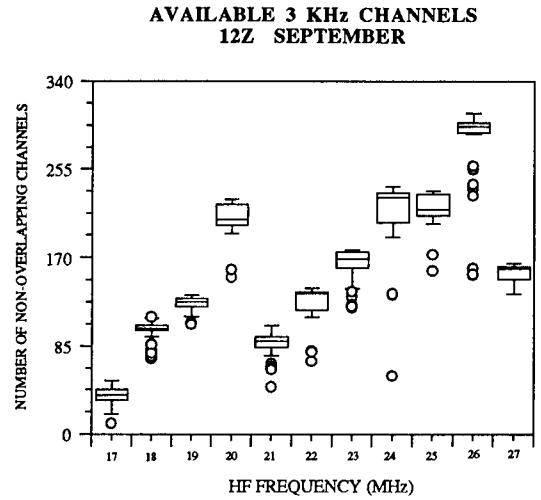
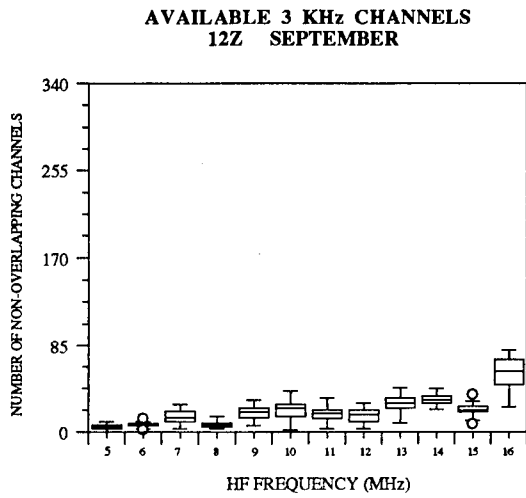


Fig. 27 — Channel Availability/September Night

The characteristics most noted from the box plots are

- (1) the bandwidth distributions for successive updates are considered to be in good agreement, which implies that the availability of bandwidths is stable;
- (2) rectangles associated with channel widths greater than 3 KHz are narrow, which implies that there are small deviations in the observed counts from update to update;
- (3) for all months considered, very few bandwidths exist above 21 KHz during the time ionospheric conditions would support ROTH signal propagation; and
- (4) January availability counts are lower and relatively uniform between 5 MHz and 16 MHz, in contrast with the other seasons which have higher availability counts and similar shapes, e.g., local peaks at 6 MHz and 9 MHz.

The characteristic identified in (4) can best be observed when the 3 KHz channel plots from each season are compared. These comparison shows that between 5 and 16 MHz, the availability count in almost all cases increases and decreases in the same frequency band for the months of April, July, and September. However, the January channel width counts for the same frequency intervals are relatively uniform in shape.

7.2 Channel Availability For Random Time Periods

The analysis and results thus far have been based on processing 20 minutes of continuous segments of SM data. However, in many instances, estimates of available bandwidth are desired over 4 hour periods. Because of computer memory limitation, processing 4 hours of continuous SM updates cannot be performed in a reasonable amount of time. Therefore, an alternative technique must be used to accomplish this task. The findings detailed in Sections 2 and 3 were used to generate arbitrary data sets of 20 minutes in length of each hour in the 4 hour period and to compute the average availability count of channel widths. This analysis was performed for the times of 00Z to 04Z and 12Z to 16Z for each of the months in this study.

Figures 28 through 31 represent the results of availability for random time periods in a condensed version of the information provided in Figs. 20 through 27. Shown in Figs. 28 through 31 are the computed averages of availability counts based on the random samples from the 4 hour data sets. Each display shows the average number of available 3 KHz, 9 KHz, 15 KHz, 21 KHz, and 30 KHz channel widths that were computed in the 5 MHz to 28 MHz frequency spectrum. The availability counts associated with these figures lie on or inside the rectangles shown in the box plots for the respective channel widths in Figs. 28 through 31. That is, the characteristics that were identified from the box plots are also present when the analysis was performed for arbitrary data sets over a 4 hour period.

Interpreting the results can be assisted by considering the information in the Fig. 10 wide sweep backscatter ionograms. Specifically, the January WSBI for 00Z (daytime) indicates that while all frequencies between 5 MHz and 28 MHz could be used, the losses are higher below 10 MHz, which may account for the lower counts when channel availability for January is compared with the other months.

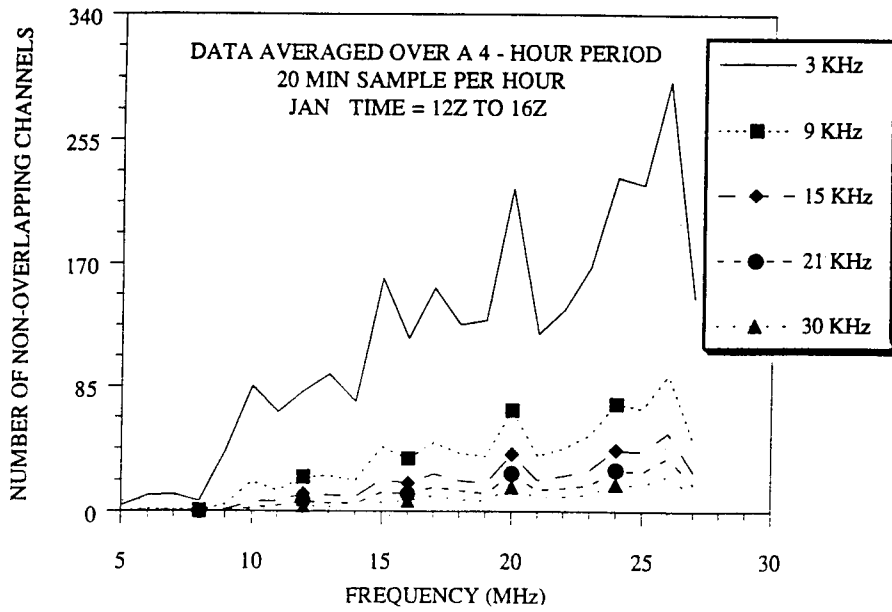
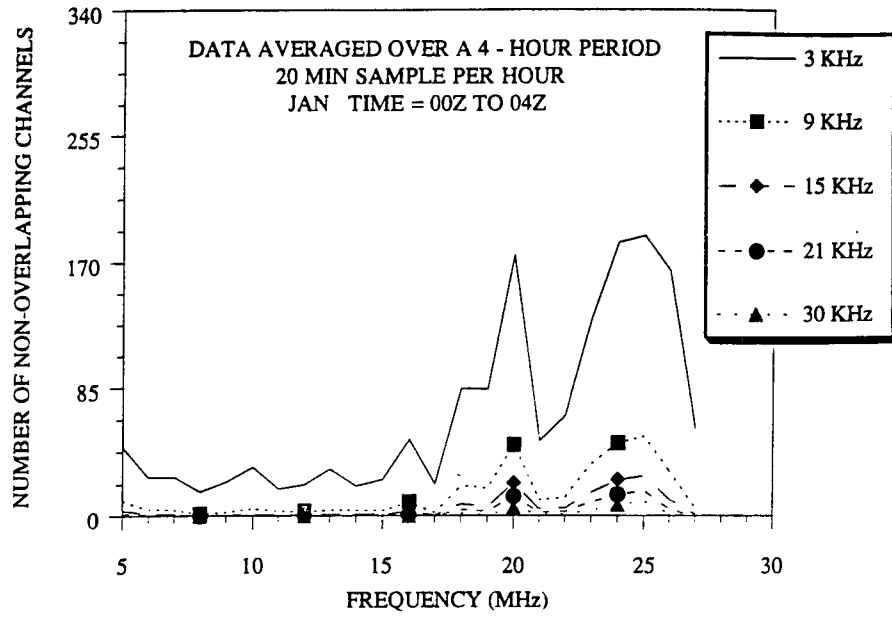


Fig. 28 — Average Channel Availability/January

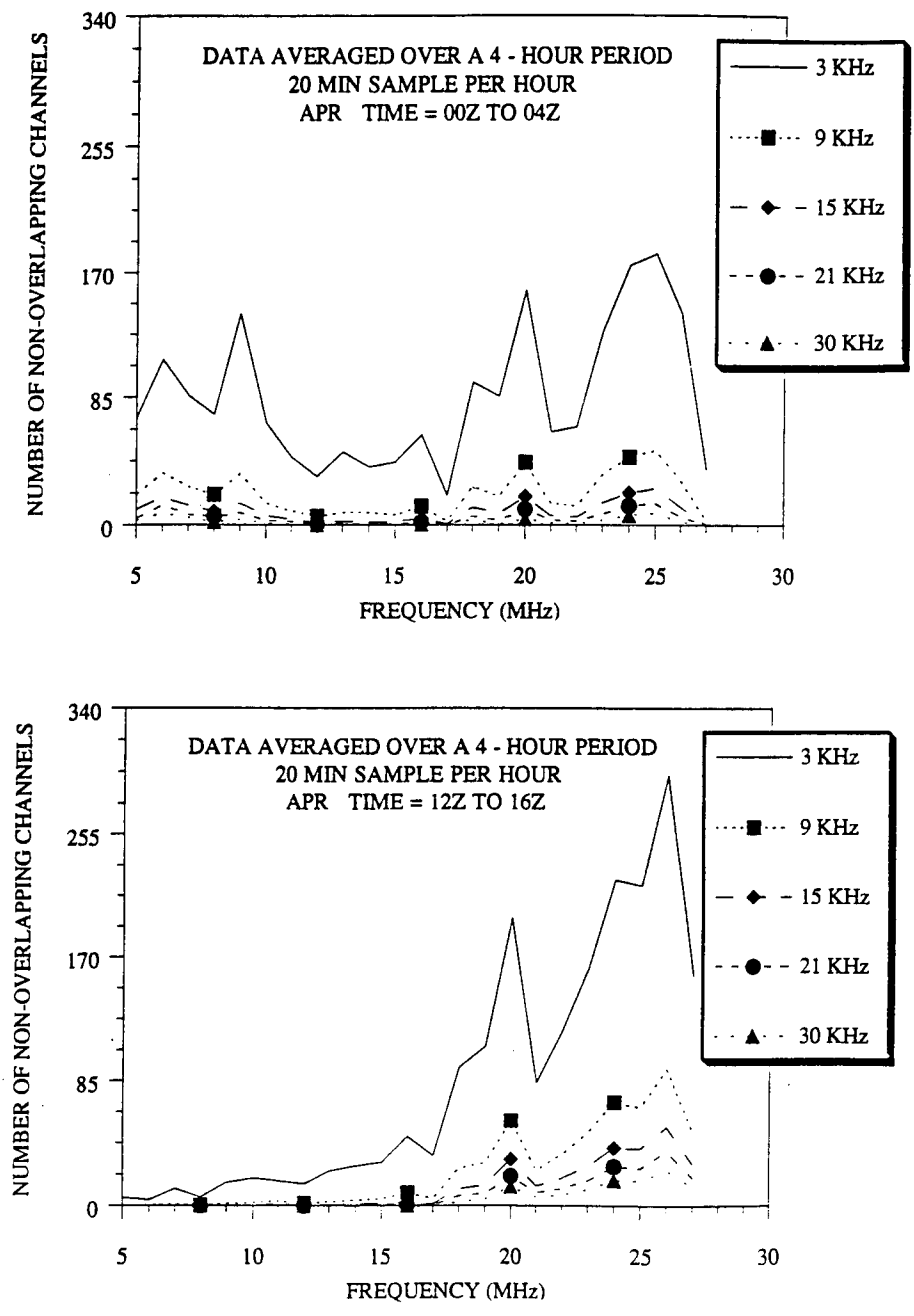


Fig. 29 — Average Channel Availability/April

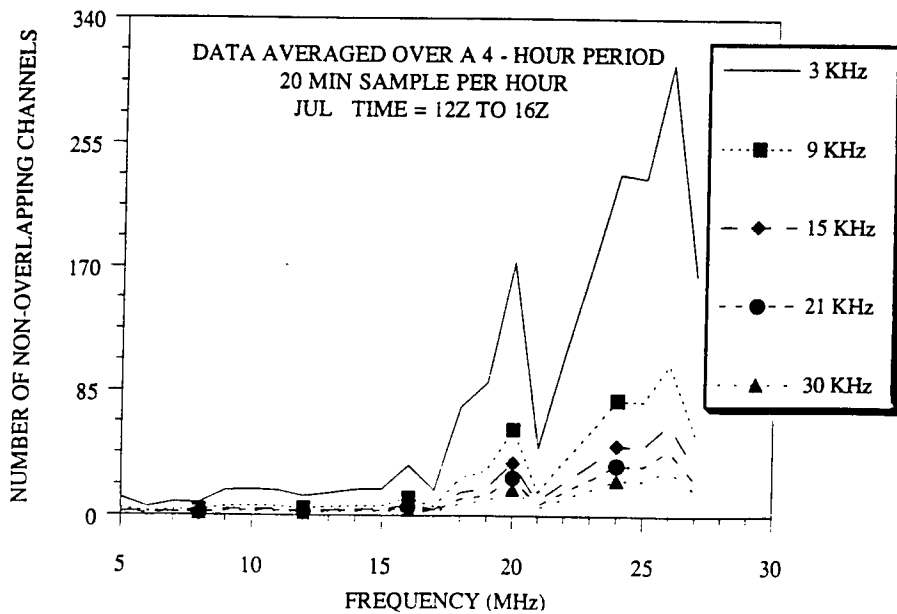
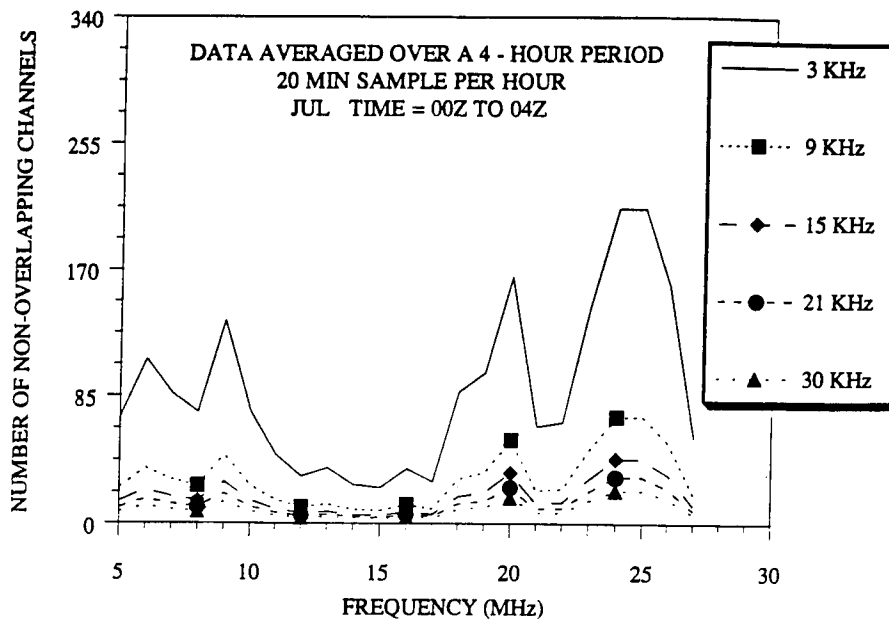


Fig. 30 — Average Channel Availability/July

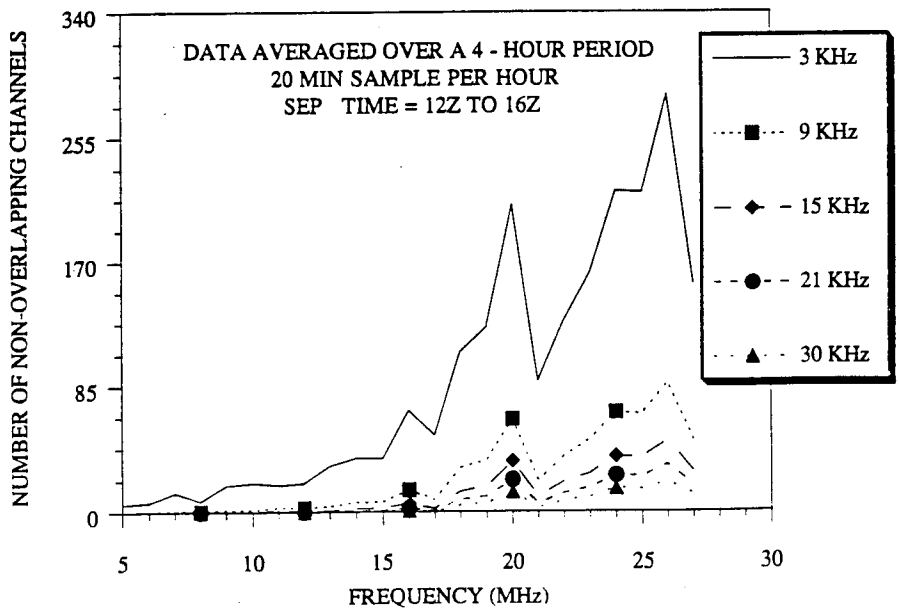
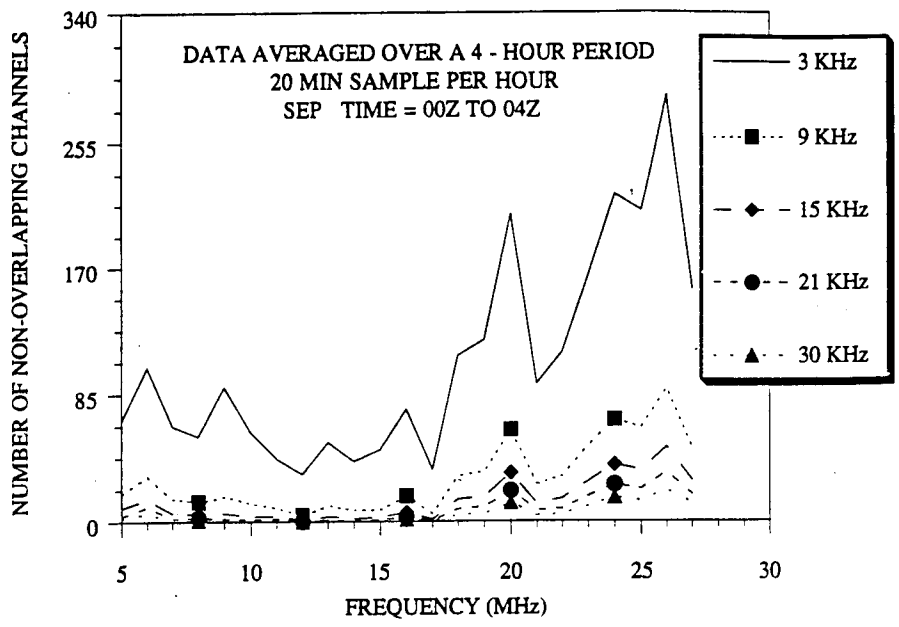


Fig. 31 — Average Channel Availability/September

8. ANALYSIS OF BANDWIDTH DURATION

In this section we investigate the duration associated with the available bandwidths discussed in Section 7. Specifically, we try to determine the number of consecutive updates that a given channel width will be available to the radar as a function of time of day, frequency, and season of the year. To obtain estimates that would provide some insight into the question, analysis of bandwidth duration was performed on the first 20 minutes of data gathered between 00Z and 12Z for the months of January and July. These months represent the winter and summer seasons, respectively. These are the seasons that will most likely indicate the most noticeable difference in channel duration. Figures 32 through 35 present the results of the analyses in the form of box plots. Because of the large number of channel widths that may be used by the radar, bandwidths of 9 KHz and 30 KHz were chosen to illustrate the duration characteristics in the data. From these bandwidths, some inferences can be made concerning other bandwidths. For example, the longest duration (run) of a 9 KHz channel implies a run of at least the same duration for all channels lower than 9 KHz, likewise for the case of a 30 KHz channel.

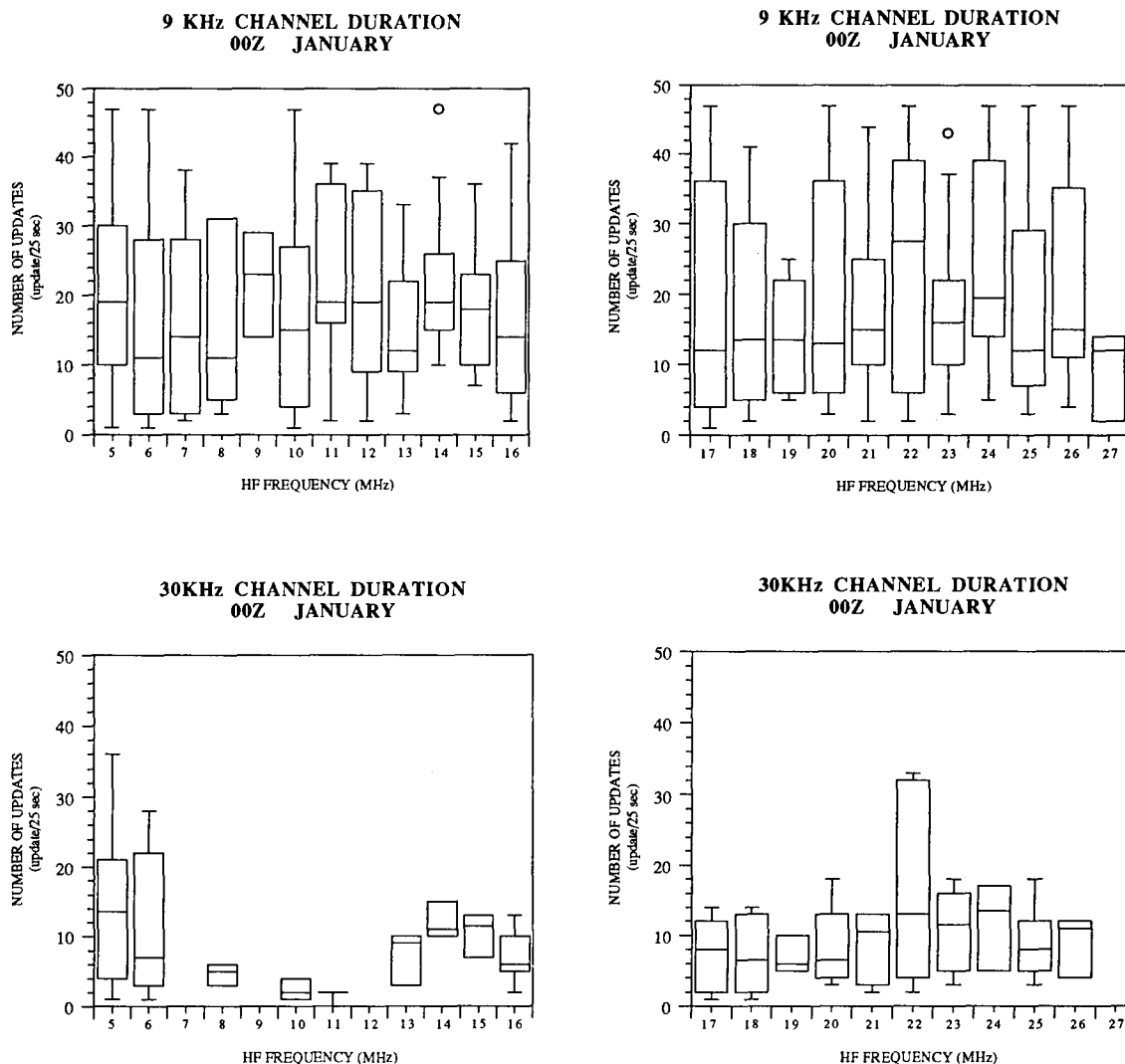


Fig. 32 — Channel Duration/January Day

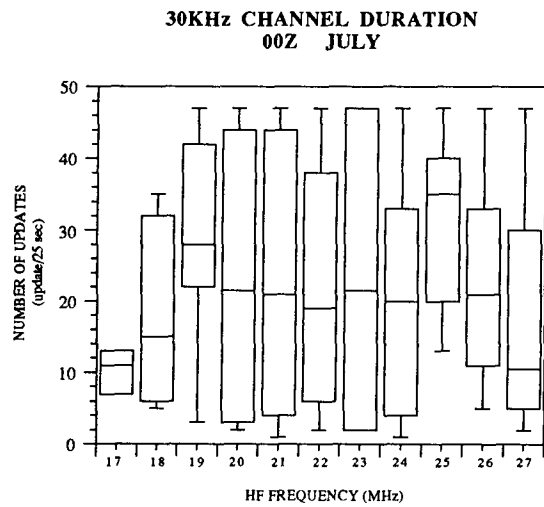
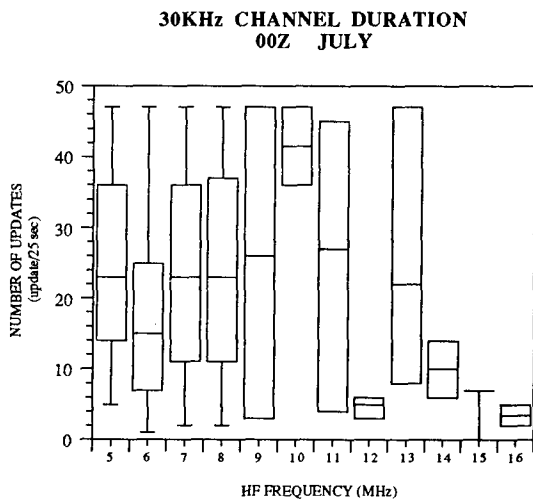
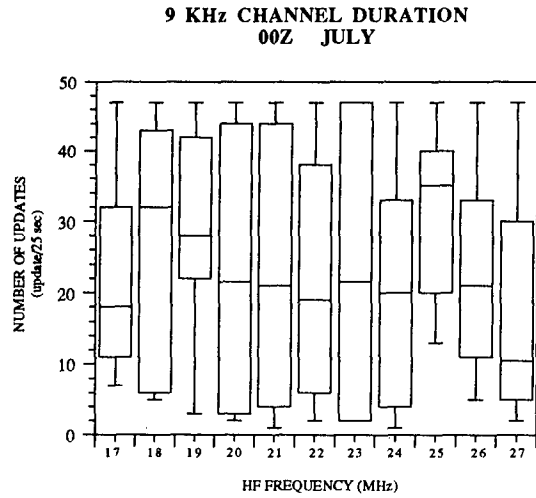
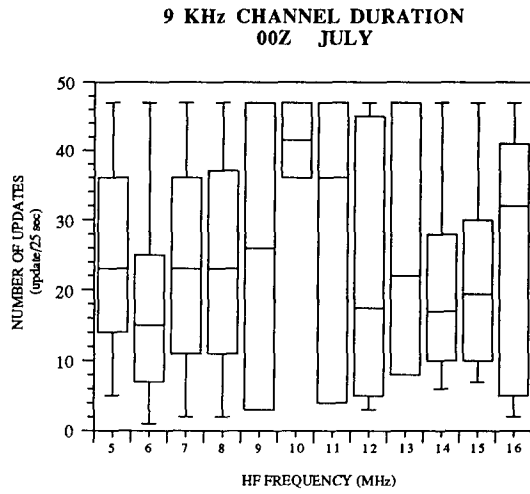


Fig. 34 — Channel Duration/July Day

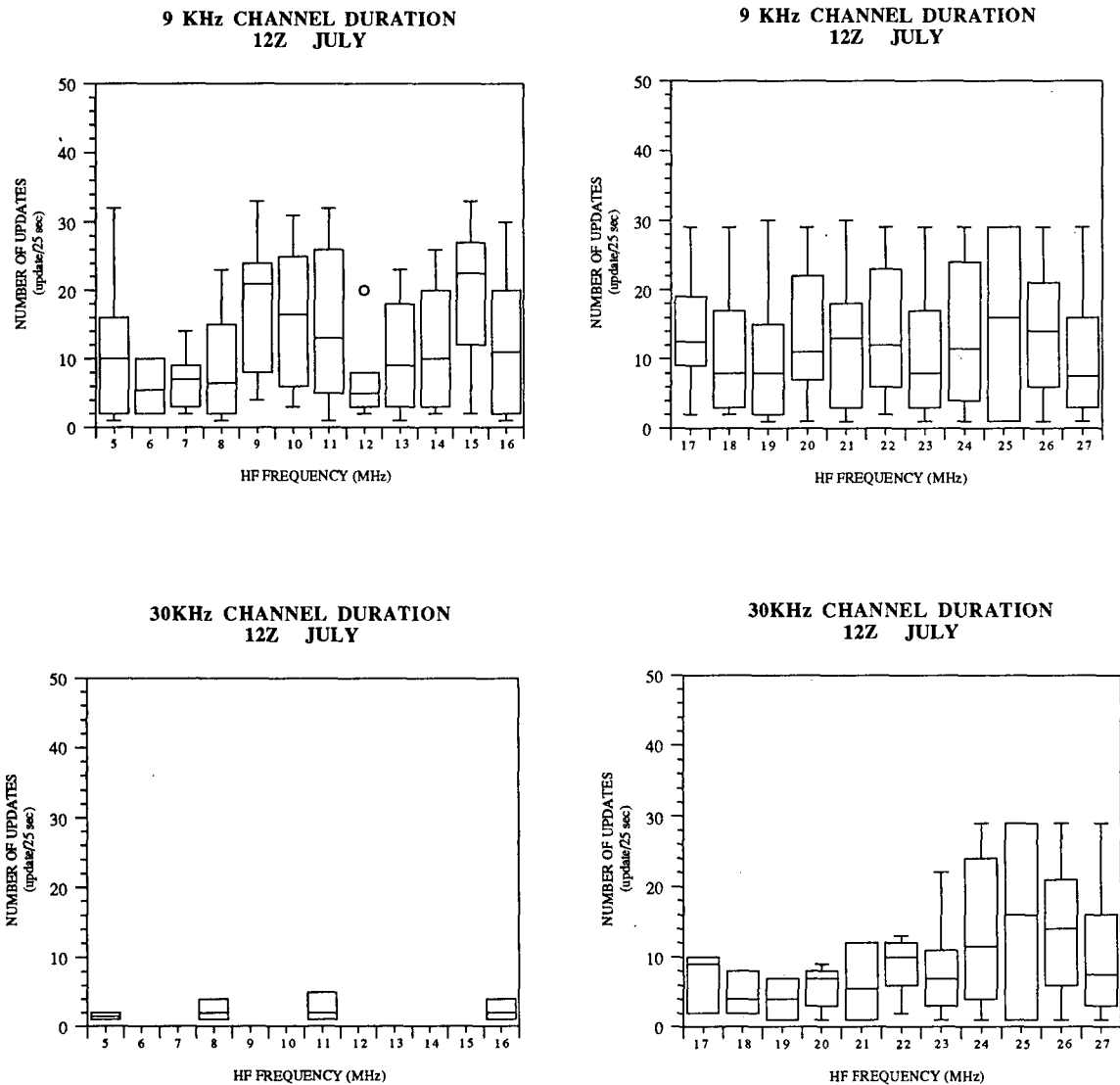


Fig. 35 — Channel Duration/July Night

Characteristics that can be observed from the box plot distributions for the months and times analyzed are as follows:

**Median Duration Range Over 5 MHz to 28 MHz
January (Winter), 00Z (Daytime)**

9 KHz 5-10 minutes (10-20 updates)	30 KHz 2-5 minutes (5-10 updates)
--	---

Figure 32 indicates frequency intervals that are most heavily occupied as observed in the 30 KHz duration plot. This observation agrees with the data presented in the bandwidth summary plot shown in Fig. 28, which also indicates few bandwidths above 30 KHz exist.

**Median Duration Range Over 5 MHz to 28 MHz
January (Winter), 12Z (Nighttime)**

9 KHz 1-7 minutes (3-15 updates)	30 KHz 1-7 minutes (3-15 updates)
--	---

Figure 33 indicates that frequencies above 8 MHz or 9 MHz are most likely not used because of ionospheric conditions, therefore we observe duration on the order of those observed during daytime hours.

The duration characteristics observed from the analysis of the July (summer) data are presented in Figs. 34 and 35, and are summarized as follows:

**Median Duration Range Over 5 MHz to 28 MHz
July (Summer), 00Z (Daytime)**

9 KHz 7-15 minutes (7-35 updates)	30 KHz 2-12 minutes (5-25 updates)
---	--

Figure 34 also shows that the most likely frequency intervals being used are between 11 MHz and 17 MHz. We note that this observation agrees with the data presented in the summary bandwidth plot for July, Fig. 30.

**Median Duration Range Over 5 MHz to 28 MHz
July (Summer), 12Z (Nighttime)**

9 KHz 2-10 minutes (5-20 updates)	30 KHz 2-5 minutes (2-10 updates)
---	---

The most noticeable difference between the summer and winter duration data for nighttime is that during the summer there are generally no 30 KHz channels with durations longer than 2 minutes for the 5 MHz to 16 MHz frequency interval. This agrees with our earlier conclusion that the bandwidths available to the radar for nighttime operation will lie below 16 MHz.

9. DISCUSSION

The development, installation, and operational deployment of the Navy's AN/TPS-71 Over-The-Horizon Radar system has provided a new source of high quality HF environmental data which in the past was not available to the HF community. The data analyzed in this study represents a small percentage of HF spectrum measurements acquired by the ROTH. However, this study demonstrates that the analysis of ROTH's SM data provides results that are in agreement with historical HF environmental data, and that these radar measurements of the spectrum are consistent and stable with respect to frequency and time-of-day. In particular, this study has shown that information concerning channel availability, channel lifetimes, characteristics of HF noise, and HF user traffic can be investigated based on the SM's measurements.

The analysis of ROTH Amchitka SM data has indicated that the radar is externally noise limited during the times when HF propagation is supported by the ionosphere, even though there were cases when the difference between the specification noise level and measured noise levels was less than zero dB. In these cases, it was noted that the behavior of the noise deltas changed as a function of frequency over the radar's operating frequency range. With respect to SM measurements vs CCIR noise predictions, atmospheric and galactic noise appear to be the major influence on ROTH noise measurements at Amchitka for both day and night cases. However, the degree of influence is seasonal and frequency dependent.

The results of this study provide an understanding of the availability of bandwidths and their duration based on actual data acquired by the ROTH radar system. In addition, the analysis techniques and programs developed during this study can be used to describe and understand many aspects of the bandwidth occupancy problem related to operating a high-frequency Over-The-Horizon Radar system in the HF spectrum. Analysis of the SM measurements has identified characteristics of the HF noise environment, the availability of free channels, and the median duration of various channel widths at the ROTH Amchitka radar site. Based on these measurements, the following characteristics were identified with respect to the indicated areas.

Amchitka's HF Environment:

- SM measurements are stable over a 60 minute time period.
- Random samples of 20 minute data sets over a 4 hour period also appear to be stable.
- The background noise can be identified by the vertical (positive, steep slope) portion of the empirical distribution of channel power levels.
- During day and nighttime hours there exist few available bandwidths greater than 21 KHz.
- Bandwidth estimates are stable and show small deviations over time for all seasons.
- Distributions of noise power levels based on SM measurements are in close agreement with noise levels seen on the radar.

Bandwidth Duration:

- Free channel durations were shorter for the winter season, for wider bandwidths and for nighttime.

Receiver Noise vs Internal Noise:

- The ROTH appears to be externally noise limited during periods when ionospheric conditions support HF propagation.

Dynamic Range:

- The difference between the maximum signal and noise level approached 100 dB.

10. ACKNOWLEDGMENTS

I wish to express my appreciation to Dr. John P. Nolan of the Department of Mathematics and Statistics, The American University, for his comments and suggestions during the exploratory data analysis phase of this project, and also I express my thanks to Mr. James M. Headrick and Mr. Joseph F. Thomason of the Radar Division of NRL for their helpful suggestions and comments on relating analysis results to radar operations.

REFERENCES

1. J. Headrick, "Looking Over The Horizon," *IEEE Spectrum* **27(7)**, 36-39, 1990.
2. H.E. Nichols and D.J. Gooding, "Probability Distributions of Received Interference Levels in the HF Band," *The Effect of the Ionosphere on Radiowave Signals and System Performance, Ionospheric Effects Symposium*, J.H. Goodman, ed., May 1-3, 1990, p. 181-188.
3. International Radio Consultative Committee (CCIR) Report 322, *World Distribution and Characteristics of Atmospheric Radio Noise, Documents of the Xth Plenary Assembly, Geneva, 1963*, International Telecommunication Union, Geneva, 1964.
4. P.C. Evans, J.M. Lomasney, W.F. Marshall, and J.R. Barnum, "OTH Radar Performance Improvement with Twin-Whip Endfire Receiving Pair (TWERP) Elements at WARF," Technical Report 36, Stanford Research Institute, Menlo Park, CA, November 1976.
5. M. Nicholas, *HF Communications (A Systems Approach)*, (Plenum Press, New York, 1987), Chap. 5.
6. L. Sachs, *Applied Statistics (A Handbook of Techniques)*, 2nd ed., (Springer-Verlag, New York, 1984).
7. R. Mason, R. Gunst, and J. Hess, *Statistical Design and Analysis of Experiments* (John Wiley & Sons, New York, 1989), Chap. 5.